Medizinische Universitätsklinik Tübingen

Aus der Abteilung Innere Medizin III –

(Schwerpunkt: Kardiologie und Angiologie)

The Assembly and Evaluation of Antisense Oligonucleotides Applied in Exon Skipping for Titin-based Mutations in Dilated Cardiomyopathy

Inaugural-Dissertation
zur Erlangung des Doktorgrades
der Medizin

der Medizinischen Fakultät
der Eberhard Karls Universität
zu Tübingen

vorgelegt von

Hahn, Julia Kelley

2021

Dekan: Professor Dr. B. Pichler

1. Berichterstatter: Professor Dr. M. Gramlich
2. Berichterstatter: Professor Dr. A. Birkenfeld

Tag der Disputation: 01.04.2021

Table of Contents

Figures

Tables

Preface

With advances in genetic diagnostics, the emphasis of disease treatment can now be more targeted and tailored to the individual genetic information of the patient, rather than the treatment focus predominantly based on a standard, applicable for a general disease for all patients. In particular, upon relatively recent completion of significant events in our understanding of human genetics, such as the event of the Human Genome Project, we now have an enormous capacity to retrieve and decipher genetic information from human tissue and cells which can help improve the way we precisely diagnose, treat and cure patients.

As physicians, one of our important duties is to strive to deliver not just adequate treatment but also offer advanced treatment options to ensure optimal therapies for each of our patients. For example, in the case of heart disease due to genetic pathological mutations, it would be desirable to offer a customized therapy for the presenting disease, where a treatment is designed based on the exact mutation found in the patient's cells.

With this perspective, the following work explores the possibility of an individualized RNA-based treatment for dilated cardiomyopathy, caused by specific mutations in the titin gene, proposing a protocol for the application of the design and the evaluation of such potential personalized gene-based therapies(Gramlich et al., 2015)(Hahn et al., 2019).

1. Introduction

1.1 The Heart and Cardiac Muscle: Basic Features and Function

1.1.1 The Heart: Basic Anatomy and Structural Features

The human heart, which provides the pumping force to deliver a dynamic and adequate, oxygen-rich blood supply to the body, while receiving and pumping deoxygenated blood forward to the lungs in a continuous cycle, is a complex internal muscular organ, located in the inferior mediastinum, situated between the anterior and posterior compartments, cranial to the diaphragm, shielded ventrally by the sternum and thoracic cage (Gavaghan, 1998).

Capable of pumping five to seven liters of blood per minute, the human heart moves through diastole and systole, representing motions of the heart cycle, triggered by the cardiac conduction system of the heart, which is comprised of a group of specialized cardiomyocytes responsible for the contraction of the heart muscle, beginning with an impulse at the sinus node followed by the atrioventricular node, bundle of His, left and right bundle branches and Purkinje fibers (Gavaghan, 1998).

As the heart pumps and passes through the actions of diastole and systole, the heart relaxes, fills with blood and contracts, respectively(Gavaghan,1998). During this time, blood moves through the four chambers and the four valves of the heart beginning with the right atrium followed by the tricuspid valve, the right ventricle, passing through the pulmonary valve, pulmonary trunk, entering in the pulmonary arteries to the lungs, and returning as oxygen rich blood back through the pulmonary veins to the left atrium, the mitral valve, the left ventricle, the aortic valve and moves forward to the aorta, wherefrom the right and left coronary arteries branch, providing the heart with an oxygen-rich blood supply, paired with a venous system returning the majority of the deoxygenated blood through the coronary sinus into the right atrium (Gavaghan,1998).

The walls of the heart are comprised of varying thickness, divided into the endocardium, myocardium, and epicardium. The pericardium encompasses the

heart; these two structures are separated by a physiological amount of fluid, providing a protective film, allowing frictionless movement (Gavaghan, 1998).

Structural changes to the normal anatomical features of the heart muscle, for example, extreme left ventricle hypertrophy or left ventricle wall thinning with enlargement of the ventricle, inevitably influence the pumping function of the heart and can thus lead to pathological function of the heart, such as heart failure with persisting structural change over time (McKenna et al., 2017).

1.1.2 Cardiac Muscle: Basic Features of The Sarcomere

Cardiac muscle belongs to the striated muscle group wherein the skeletal muscle is also found. The cardiac and skeletal muscle differ majorly from the third muscle group, the smooth muscle, by the presence of the sarcomere, a distinctive feature of the striated muscle group (Squire, 1997).

The sarcomere is the smallest functional unit of the striated muscle tissue, which is aligned in a repeating order in the tubular myofibrils. Each sarcomere is formed by portions of the gliding myofilaments, namely the thick myosin and thin actin myofilaments(Squire, 1997). The sarcomere is further organized in distinctive bands, zones and lines, marking specific sections of each sarcomere. The repetitive I-band and A-bands create the striations observed upon polarized microscopy. The I-band, located at the periphery of each sarcomere, is comprised of actin filaments alone. Here the actin filaments are anchored to the Z-lines, the portion of the sarcomere where it is defined that each sarcomere begins and ends; two Z-lines closest in proximity to each other mark a singular sarcomeric unit(Squire, 1997). Adjacent to the I-band is the A-band, comprised of the three smaller units which includes a central H-zone containing a myosin myofilament zone in the absence of actin, the M-line, marking the middle of the H-zone, where the myosin filaments are anchored. In addition, the myofilaments actin and myosin on each side of the central H-zone are organized in a parallel

order. In this region there is myosin head formation, crucial for muscle contraction (Squire, 1997).

During the action of muscle contraction, a well investigated mechanism involving the interaction of ATP (Adenosine triphosphate), ATPase activity, and calcium and tropomyosin, the myofilaments slide along each other bringing proximally positioned Z-lines closer in distance to one other as the I-band and H-zone shorten temporarily in length. A crucial protein provides the returning force of the sarcomere to its starting position, namely, the giant sarcomeric protein, titin (Squire, 1997).

The structural, sarcomeric protein titin is an essential contributor to the physiological function of the sarcomere(Gramlich et al., 2015). Titin spans from the M-line to the Z-line, acting as a spring-like component of the sarcomere, aiding in its return to the pre-contraction position, providing limitation to the passive stretch of the sarcomere(Squire, 1997)(Gramlich et al., 2015). Detailed features of titin and mutations in the TTN gene and its relevance to development of DCM (Dilated Cardiomyopathy) are a core focus of this dissertation further elaborated in Section 1.2.3.

1.2 Structural Changes to the Heart: Cardiomyopathies and Dilated Cardiomyopathy

1.2.1 Cardiomyopathies: Definition and Classification

Cardiomyopathies, in their most simple described definition, are cardiac muscle diseases (McKenna et al., 2017). However, predominantly beginning in early 1980s, the definition of cardiomyopathies continues to be updated, partly in efforts to more precisely exclude or include different factors and etiologies contributing to the formation of the disease.

For example, in 1980, The World Health Organization (WHO) aimed at refining the definition of cardiomyopathies, attempting at excluding cardiovascular factors which could potentially lead to dysfunction of the heart and thus, lead to cardiomyopathy, such as hypertension or valvular disease; here the definition

was proposed as “heart muscle diseases of unknown cause” (Report of WHO, 1980). As this definition proved to be limited in its application in a clinical setting, further adjustments to the definition took place.

More recent definitions with corresponding detailed classification systems are provided by the American Heart Association (AHA) and the European Society of Cardiology (ESC). In 2006, the AHA stated, *“Cardiomyopathies are a heterogeneous group of diseases of the myocardium associated with mechanical and/or electrical dysfunction that usually (but not invariably) exhibit inappropriate ventricular hypertrophy or dilation and are due to a variety of causes that frequently are genetic. Cardiomyopathies either are confined to the heart or are a part of generalized systemic disorders, often leading to cardiovascular death or progressive heart failure-related disability"* (Maron et al., 2006). Two years following this statement, in 2008, the ESC proposed the following definition, which proved to be more useful in determining a clinical diagnosis, which states cardiomyopathies are *“a myocardial disorder in which the heart muscle is structurally and functionally abnormal in the absence of coronary artery disease, hypertension, valvular disease and congenital heart disease sufficient to explain the observed myocardial abnormality"* (Elliott et al., 2008). As new discoveries involving the etiology of cardiomyopathies are made, the definition is expected to continue to evolve.

Among the different types of cardiomyopathies, the focus of this work involves a specific genetic mutation causing *dilated cardiomyopathy*. It is, however, essential to initially emphasize the many entities that comprise the entire body of the disease which is defined by cardiomyopathies, as there are overlapping etiologies and genetic mutations leading to variable types of cardiomyopathy. Although a discussion of the general overview of the cardiomyopathies is also possible using the ASH proposed classification, here the ESC classification of cardiomyopathies is further elaborated for simplicity purposes (Elliott et al., 2008).

According to the ESC proposed classification of cardiomyopathies, there are five core types of the disease: hypertrophic cardiomyopathy, dilated

cardiomyopathy, arrhythmogenic right ventricle cardiomyopathy, restrictive cardiomyopathy, and unclassified cardiomyopathy(Elliot et al., 2008). These five types are further divided into two subgroups: familial/genetic and non-familial/non-genetic; these two subgroups are further divided into the following, respectively: unidentified gene defect and disease subtype, and idiopathic and disease subtype (Elliot et al., 2008). The authors of this work emphasize the major change in the proposed classification system shifts classification of the disease from previously implemented "diagnosis by exclusion" and brings heart function and morphology to focus, in attempts to underscore the abundant etiologies of the disease for easier application in a clinical setting (Elliot et al., 2008).

For example, in clinical practice a direct application of the ESC proposed classification of cardiomyopathies would translate to promptly seeking the answer to the following: is the suspected cardiomyopathy most likely genetic or not(Elliot et al., 2008)? In order to best answer this question, information is gathered from patient history, clinical examination and diagnostic heart testing (electrocardiogram (ECG) and echocardiography). In some cases, additional testing for suspected genetic mutations potentially causing the cardiomyopathy can also be performed (Elliot et al., 2008).

1.2.2 Dilated Cardiomyopathy and Genetic Mutations

"*Dilated cardiomyopathy is a structural heart disease distinguished by left ventricular dilation and systolic dysfunction; it is a primary cause for progressive heart failure with prevalence up to 1:250 (Hershberger et al., 2013). A specific treatment option for patients with DCM other than heart transplantation does not currently exist" (*Hahn et al., 2019).

Upon considering the different categories of dilated cardiomyopathy according to the above mentioned ESC proposed classification, DCM is classified into the following: familial dilated cardiomyopathy and nonfamilial dilated cardiomyopathy (Elliot et al., 2008). It is also of relevance to note, however,

dilated cardiomyopathy can also additionally be classified as idiopathic, where most common causes of the disease are ruled out. In some cases, for example, nonfamilial DCM can be classified as idiopathic. However, as most idiopathic cases are classified excluding genetic causes, it is not uncommon for a familial dilated cardiomyopathy to be initially categorized as idiopathic in a clinical setting in which a genetic mutation leading to the disease is not yet detected. Idiopathic dilated cardiomyopathy is, among all types of cardiomyopathies, the major indication for heart transplantation (Manolio et al., 1992).

Dilated cardiomyopathy is a disease caused by a diverse group of etiologies. These include but are not limited to the following: ischemic heart disease (e.g. coronary heart disease) , stress-induced cardiomyopathy, infectious disease (e.g. adenovirus, coxsackie virus, Streptococci-rheumatic fever, syphilis, cryptococcosis, toxoplasmosis), medications (e.g. Anthracyclines, Zidovudine, Clozapine), inflammatory or autoimmune processes (e.g. Systemic lupus erythematosus, sarcoidosis, Kawasaki disease), toxins (e.g. ethanol, cocaine, lithium), endocrinologic dysfunctions (e.g. Diabetes mellitus, pheochromocytoma), electrolyte and nutritional imbalance (e.g. hypocalcemia, Thiamine deficiency), deposition diseases (e.g. amyloidosis, hemochromatosis), variable other causes(e.g. tachycardia, hypothermia, peripartum cardiomyopathy) as well as genetic diseases (e.g. familial or sporadic, Duchenne muscular dystrophy) (Weigner et al., 2019).

Genetic mutations associated with dilated cardiomyopathy are nearly as abundant as the primary etiologies of the disease mentioned above. Furthermore, novel findings continue to be discovered pertaining to these mutations with variations in gene mutation location, type and impact on disease formation (Weigner et al., 2019). Currently, a general understanding of the genetic causes of DCM are established, including distinct mutations in genes believed to largely contribute to the disease process in dilated cardiomyopathy.

Overall, in considering mutations linked to familial dilated cardiomyopathy (FDC), there are greater than thirty autosomal genes and two x-linked genes contributing to and influencing the formation of the disease in diverse genetic

processes (Hershberger 2019). Many of the identified autosomal mutations exhibit autosomal dominant inheritance. Although this is a seemingly high number of mutations identified, at this time it is believed that the known mutations comprise roughly 50% of the genetic mutations contributing to FDC (Hershberger 2019).

The genetic mutations linked to FDC are categorized by Hershberger in various ways, including according to inheritance pattern, mechanism of disease development as well as gene specific "*estimated fraction of DCM,"* providing a type of impact factor for a given identified gene and its relevance in FDC (Hershberger 2019). Further discussion of the genetic mutations linked to FDC will provide an overview of not all but highly relevant identified mutations pertaining to this paper.

To begin, upon considering DCM with or without features such as conduction system disease, "*by far the most common phenotype is DCM without accompanying distinctive features (in common practice, >90 to 95 percent*)" (Hershberger 2019). Mutations in sarcomere genes are included in this designated category of FDC described by Hershberger, whereby approximately 30% of FDC cases are included; the following are examples of mentionable sarcomere genes involved in FDC: alpha myosin heavy chain (MYH6), beta myosin heavy chain (MYH7), cardiac troponin T (TNNT2), alpha-tropomyosin (TPM1), cardiac troponin C (TNNC1) and titin (TTN) (Hershberger 2019). The MYH7 gene encodes the beta myosin heavy chain protein, which is present in both cardiac and skeletal muscle, providing an essential role in muscle contraction; mutations in MHY7 are a common cause of FDC with an estimated fraction of DCM of 0.04 (Hershberger 2019). In addition, mutations in the MYH7 gene are not only associated with FDC but are also linked to the formation of hypertrophic cardiomyopathy (Hershberger 2019). Mutations in the TNNT2 gene, responsible for cardiac troponin T, a protein playing an important role in regulation of the thick and thin calcium modified filament interaction, are noted to often exhibit a phenotype presenting earlier in life, with an exceptionally severe clinical pathology (Hershberger 2019).

Although the most common mutations linked to FDC involve the sarcomere genes, there are also non-sarcomere genes with associated conduction system pathologies (LMNA), x-linked genes(dystrophin) and syndromes(Barth's syndrome), autosomal recessive genes(ALMS1) and as well as other rare disorders in mitochondrial DNA which cause FDC (Hershberger 2019). For example, mutations in the x-linked dystrophin gene most commonly contribute to the formation of dilated cardiomyopathy; the majority of mutations in the dystrophin gene are known to cause Becker muscular dystrophy or Duchenne muscular dystrophy, both of which can not only produce pathological formation of the skeletal muscle but also cardiac muscle (Hershberger 2019).

Nonetheless, among all sarcomere genes and non-sarcomere genes known to cause Dilated Cardiomyopathy, the most common contributing factor to the disease formation in FDC are mutations in the TTN gene (Herman et al., 2012).

1.2.3 Dilated Cardiomyopathy and Mutations in the TTN gene

"To date, over forty genes are linked to and associated with DCM (Tayal et al., 2017). However, truncating variants in the TTN gene dominate as the major cause of genetically related DCM, accounting for approximately 15-20% of familial DCM cases (Tabish et al., 2017)(Herman et al., 2012) (Roberts et al., 2015). Titin-truncating variants (TTNtv) are also carried by 1% of the general population (Schafer et al., 2017). Such mutations in the TTN gene ultimately lead to altered titin protein synthesis which is shortened in sequence length and render subsequent complications in essential cell function such as sarcomerogenesis as well as protein interactions (Gramlich et al., 2015)" (Hahn et al., 2019).

Titin, the protein encoded by TTN, is *"a giant sarcomeric protein that stretches half of the cardiac sarcomere, which among various functions, provides crucial myofibril elasticity and guides sarcomeric assembly. Within a single TTN gene there are 363 exons, thereof 90% harboring repeating modular immunoglobulin-C2 (Ig-C2) and fibronectin-III(Fn-III) domains, consisting of protein binding sites*

for myofibrillar proteins; the remaining 10% of the TTN gene is comprised of non-repetitive regions consisting of other modular structures such as phosphorylation motifs and serine/threonine kinase domains (Kontrogianni-Konstantopoulos et al., 2009). Upon considering hot spots of the TTN transcript associated with relevant mutations, the largest number of TTNtv are located in the inextensible A-band region of the sarcomere, including the TTN truncating mutations examined(Roberts et al., 2015)" [in this dissertation] (Hahn et al., 2019).

In order to consider the pathogenesis of titin-based DCM, additional functional features of titin should be discussed. TTN encodes various isoforms of titin, these include varying degrees of elasticity and stiffness, allowing for alternate compositions of the protein for optimal functionality in specific tissue such as the heart, where the titin isoform presents with different I- band lengths following alternate splicing (Garfinkel et al., 2018). Titin also harbors four functional domains: 1) the M-band functional domain, rich in kinase with links to protein signaling 2) the I-band functional domain, providing "passive tension" limiting the sarcomere in its ability to stretch and to restore resting state 3) the Z-disc functional domain, providing the region of assembly of the myofibril 4) the A-band functional domain, recently reported as the location of the most TTNtv, is a region where vital myosin protein binding occurs (Herman et al., 2012) (Garfinkel et al., 2018). Hence, the protein interaction titin performs is tremendous, with alteration to these processes possibly leading to the malfunction of the cardiac sarcomere and thus, to the heart.

The genetic inheritance pattern of TTNtv are categorized as autosomal dominant and tend to not present with accompanying conduction system malfunction (Hershberger 2019). The TTNtv most commonly present as nonsense mutations but are also known to present as various forms of mutations, such as base pair insertion or deletion mutations causing frameshift mutations as observed in the investigated TTN mutation in this study. The clinical manifestation of TTNtv are unfortunately unspecific, where most patients are initially diagnosed with idiopathic dilated cardiomyopathy; it is, however reported, severer forms of the disease may occur in men rather than women

(Hershberger 2019). These unspecific features produce a challenge in the identification of the mutation, leaving patient and family history(first-degree relatives, up to fourth generation family history) as well as general cardiac diagnostics (transthoracic echocardiography, ECG, serum parameters) important indicators for subsequent genetic testing.

The pathogenesis of titin-based DCM is multifaceted and not yet fully understood. It is clear most of the TTNtv contributing to DCM are located in the A-band region; however, why these mutations are concentrated in this region remains unclear (Garfinkel et al., 2018). In addition, TTNtv are thought to cause haploinsufficiency, reduce sarcomerogensis, as well as cause reduction of the "passive stiffness" in cardiac muscle, yielding exacerbated sarcomere stretch, producing less sarcomere force (Garfinkel et al., 2018). In the case of TTNtv causing frameshift mutations in the A-band region, these mutation are described as causing truncated versions of titin and thus altering protein function and sarcomerogensis, ultimately leading to systolic dysfunction and eventually to the clinical presentation of DCM (Gramlich et al., 2015). It is also relevant to note, a positive genotype does not guarantee a positive phenotype with regards to TTNtv, as up to 2% of the general population carry TTNtv without clinical manifestation, which may, however, play a role in the presence of additional stressors in acquired DCM (Garfinkel et al., 2018). Despite the etiology of the disease, DCM is currently treated with evidence-based guidelines, according to clinical manifestation and severity of disease.

1.3 Dilated Cardiomyopathy: Treatment

DCM is a major cause of heart failure and the disease, upon symptom presentation, is treated as such; evidence-based therapy guidelines for heart failure diagnosis and treatment are published among multiple countries throughout the world with reported minimal difference in common recommendations, for simplicity purposes, the guidelines published in 2016 according to the European Society of Cardiology (ESC) will be referenced to,

upon considering detailed therapeutic approaches in this dissertation (Hershberger 2019) (Ponikowski et al., 2016).

DCM treatment is based on “cardiac phenotype” and the established heart failure therapy (Hershberger 2019). This therapy mostly aims at improving symptoms, reducing frequency in hospitalization, preserving heart ventricular pump function and increasing life quality; currently, the only complete curative therapy for advanced-stage DCM is heart transplantation, a therapy with extreme limited availability (Hershberger 2019). According to the Heart Failure Society of America (2009), the treatment for familial DCM, with identification of a related genetic mutation, does not drastically alter the a patient’s general DCM treatment plan; thus, the treatment for familial DCM does not dramatically differ from the non-familial DCM cases (Hershberger 2019). However, there are some differences involving advanced care, such as considering time of indication for primary preventative devices such as implantable cardiac defibrillators and unique situations involving syndrome-related DCM, where additional syndrome-specific therapy approaches are necessary(Hershberger 2019).

Upon confirmation of the diagnosis of DCM and subsequent confirmed heart failure diagnosis, treatment can be overall categorized as seen in the 2016 ESC Heart Failure Therapy Guidelines in the following: 1) pharmacological therapy and 2) device therapies(Ponikowski et al., 2016). Treatment is further categorized in considering “preserved, mid-range and reduced ejection fraction” (Ponikowski et al., 2016). Pharmacological therapy includes a vast spectrum of medication (e.g. Beta-blockers, angiotensin-converting enzyme inhibitors, angiotensin receptor blockers, angiotensin receptor neprilysin inhibitors, hydralazine and isosorbide dinitrates, mineralocorticoid receptor antagonists, ivabradine, diuretics, oral anticoagulants and antiplatelet therapies, 3-Hydroxy-3-methylglutaryl-coenzyme A reductase Inhibitors and Digoxin), which is implemented in a step-wise regime, considering a) presenting persisting symptoms, further classified using the New Year Heart Association (NYHA) heart failure classification and b) observed ejection fraction (Ponikowski et al., 2016). For example, according to the ESC Guidelines, initial pharmacological

therapy would begin when a patient presenting with heart failure with typical symptoms; here, an initial combination therapy with a beta-blocker and angiotensin-converting enzyme inhibitor would be administered and continued until the maximum recommended dosage is achieved(Ponikowski et al., 2016). From this point, considering persisting symptoms and ejection fraction, an escalation of the heart failure therapy can further be modified with the addition of a diuretic therapy and additional pharmacological therapies, considering the patient's symptoms and response to previous treatment. Device therapy (e.g. cardiac resynchronization therapy and implantable cardioverter defibrillators) is an additional category of heart failure treatment, where in cases such as patients with, for example, risk of sudden cardiac arrest, life-threatening arrhythmias and severely reduced ejection fraction, which play an important role in the management of the disease (Ponikowski et al., 2016). Further end-stage disease therapies consist of the left ventricular assist device (LVAD) and ultimately, the indication for heart transplantation. Implantation of an LVAD involves interdisciplinary advisory for therapy indication with lengthy patient evaluation; however, the device can offer a "bridge to therapy" or even "destination therapy" as an alternate therapy for patients with few end-stage disease alternatives (Ponikowski et al., 2016).

Thus, when considering familial DCM, alternate therapeutic options would be highly deseriable, where focus on the unique genetic mutation causing the diesease could lead to a novel therapuetic approach which not only relieved symptoms but could possibly halt disease formation; this disseration explores such an approach, specifically in the scope of exon skipping in titin-based DCM.

1.4 AON-Mediated Exon Skipping in Titin-Based DCM: An Alternative Therapeutic Approach

In the last two decades tremendous research has been conducted on advances in molecular and genetic therapeutic approaches in disease treatment. In particular, the method of *exon skipping* first emerged in the mid-1990s with initial research conducted on mutated exons associated with the muscular

dystrophy disorder, Duchenne Muscular Dystrophy (DMD) (Aartsma-Rus et al., 2009). The exon skipping method is a technique which aims to “skip” or alter gene expression by “skipping” a mutated exon during transcription, resulting in a functionally intact protein with the desired exclusion of a targeted mutated exon (Aartsma-Rus et al., 2009).

Exon skipping technology is originally based upon implementing Antisense-Oligoribonucleotides (AONs) with specific qualities to enable skipping of a targeted exon(Aartsma-Rus et al., 2009). Here, the AONs are RNA fragments with an average length of 20-30 base pairs constructed of the complimentary sequence to a region of the mutated exon called, “Exonic Splicing Enhancer” (ESE) sequences. ESE sequences are detectable throughout a targeted mutated exon and play an important role in normal processes of splicing during transcription; these sequences are also necessary for the integration of an exon in mature mRNA(Aartsma-Rus et al., 2009). The complimentary sequence of the designed AONs to the mutated exon’s ESE sites is essential for successful exon skipping; the AONs bind to these sites and prevent sequence recognition of the splicing apparatus, leading to desired exclusion of the targeted exon in the transcript (Aartsma-Rus et al., 2009)(Gramlich et al., 2015). There are currently numerous designed AONs developed and tested for mutations associated with genetic diseases.

Upon considering DMD, there are AONs successfully designed for all 79 exons of human Dystrophin (Wilton et al., 2007). Here, exon skipping strategies have reached the phase of clinical trials, including two pharmacological therapies receiving US Food and Drug Administration approval. For example, *“in 2016…the FDA approved the drug Eteplirsen (Exondys 51) in treatment for DMD, designed to cause exon skipping in the DMD gene(Syed, 2016) (Echevarria at al., 2018)”* (Hahn et al., 2019). Taken together, these results indicate promising potential application of such a therapy in other genetic diseases associated with mutated exons.

Exon skipping in titin-based DCM has proven successful in cell and small animal models (Gramlich et al., 2015). In particular, previous work in AON-

mediated exon skipping was conducted, where the authors *"investigated the first identified human TTN mutation known to have a genetic-basis in DCM… the titin truncating mutation in exon 326 which causes a frameshift due to a 2-bp insertion (Gramlich et al., 2015)"*(Hahn et al., 2019). Here, exon skipping was implemented using AONs designed to block the ESE sequences of the TTN exon 326 with the aim of "skipping" the mutated exon, ending with a shortened but functional protein (Gramlich et al., 2015). AONs were initially investigated in the HL-1 mouse atrial cardiomyocyte tumor cell line with subsequent studies in a mouse model as well as induced pluripotent stem(iPS) cells-cardiomyocytes from a patient known to harbor a TTN Exon 326 mutation; the study schema of this investigation is depicted in Figure 1.0 (Gramlich et al., 2015). Results from the HL-1 cell studies indicated designed AONs enabled successful target exon skipping on the mRNA and protein level, with no indication of detrimental effects to structure or function of the cardiomyocytes. The designed AONs were further tested on iPS-cardiomyocytes as mentioned above; results confirmed successful exon skipping and showed that restoration of the reading frame contributed to improved organization of the sarcomere as well as contractility of the iPS-cardiomyocytes(Gramlich et al, 2015). Finally, it was shown in mouse models that with the designed AON treatment, the development of DCM could be prevented in adult heterozygous Titin knock-in mice (Gramlich et al, 2015).

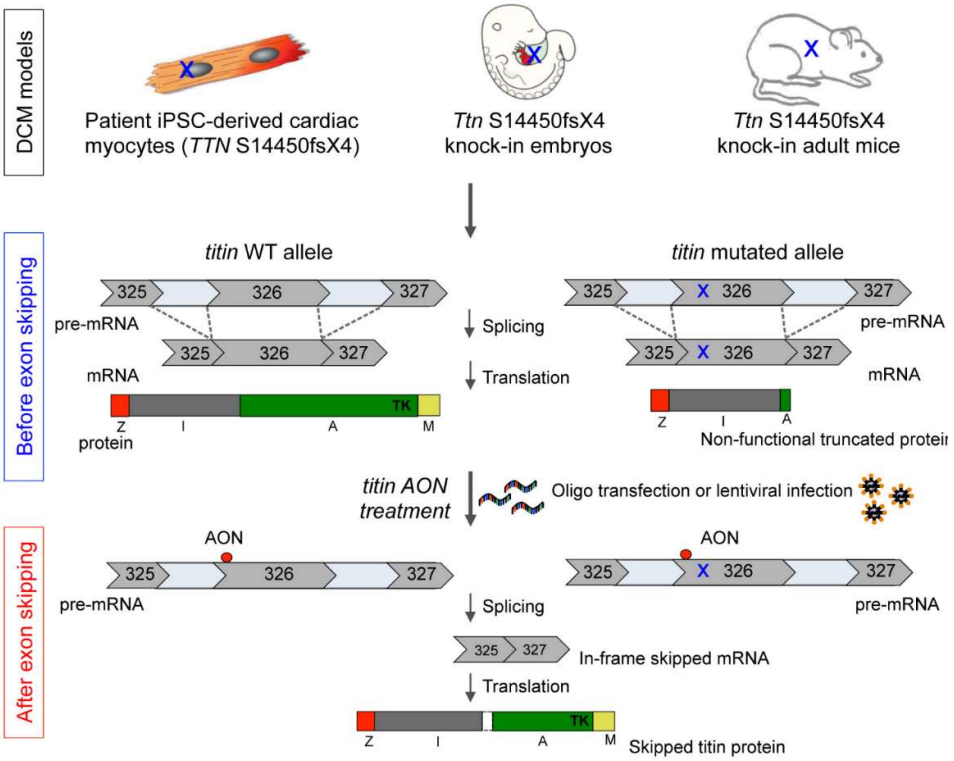

Figure 1.0: Exon Skipping Strategy in The Treatment Approach of Titin-based DCM

Antisense-Oligonucleotides lead to exon "skipping" of the mutated exon harboring a frameshift mutation, TTN Exon 326. This results in restoration of the reading frame, producing a "*shortened, but functional protein*"(Gramlich et al., 2015). The exon skipping strategy was evaluated in induced pluripotent stem cells from a patient with an identified TTN Exon 326 mutation. In addition, this strategy was also evaluated in a mouse model (Gramlich et al., 2015). *Original graphic from Gramlich et al., 2015; permission to display granted by Univ.-Prof. Dr. med. Michael Gramlich.*

1.5 Design of AON Sequences in Exon Skipping

"To date, there are over 400 AONs designed for the DMD gene; however, for other genes such as TTN, very few AONs are established (Aartsma-Rus, 2012). The massive amount of potential mutant target exons in TTN provide a challenge to address; each mutation requires the appropriately designed and evaluated AON or correct combination of AONs to preform adequate exon skipping. Previously published recommended guidelines on designing AONs for exon skipping studies are primarily focused on target exons involving the DMD gene and other mutated exons related to muscular dystrophies(Aartsma-Rus, 2012)(Pramono et al., 2012)(Shimo et al., 2018)" (Hahn et al., 2019).

1.6 Aim of Study

In this dissertation, a protocol is proposed *"that firstly successfully applies published guidelines to developing AONs for a TTN target exon, specifically in [this] investigation, the TTN exon 335; secondly,…a method of validation and evaluation of AON mediated exon skipping in treated HL-1 cardiomyocytes, to ensure retained cell functionality [is provided]. Furthermore, the proposed method is expected to be applicable to developing further AONs for emerging TTNtv, expanding the possibility of an AON mediated exon-skipping therapy in titin-based DCM"* (Hahn et al., 2019).

2. Material and Methods

2.1 Sequence Design of Antisense Oligonucleotides

"Antisense oligonucleotides (AONs) are known to be able to hybridize to a sense target sequence, causing a modulation of pre-mRNA splicing to induce exon skipping. In the presence of a missense variant, exon skipping can restore the reading frame leading to a more functional protein compared to the mutant (Aartsma-Rus, 2012).

The human TTN exon 335, previously identified as possessing a 1-bp deletion mutation, was selected as the target for our exon skipping studies (Gerull et al., 2006). For experimental purposes, the corresponding Ttn mouse exon sequence was identified, confirmed by sequence analysis and employed in the antisense oligonucleotide design process" (Hahn et al., 2019). This was completed by searching the Ensembl (ensembl.org) database for the matching exon *Ttn* mouse nucleotide sequence. The correct correlating *Ttn* exon was confirmed by sequence analysis and employed in the antisense oligonucleotide design process. *"The AONs were designed overall by combining overall recommended guidelines and our preferred chemistry, shown in our previous work to produce successful exon skipping in the TTN exon(Aartsma-Rus, 2012) (Gramlich et al., 2015). The following detailed steps were employed in designing two AONs targeting the Ttn exon 335: (1) the secondary structure of the chosen exon was constructed using the RNAstructure Web Server (http://rna.urmc.rochester.edu/ RNAstructureWeb/) (Aligam, 2017)"* (Hahn et al., 2019)*;* predict a secondary structure was selected. *"The first 50 nucleotides of the preceding Ttn intron 334 and the first 150 nucleotides of Ttn exon 335 were manually entered into the sequence box. Nucleic acid type RNA, default settings and submit query were selected. Upon viewing the generated secondary structure, partially open and closed structures located closest to the starting region of the exon were noted. (2) Exonic splicing enhancer motifs (ESEs) were identified using the Human Splicing Finder software, version 2.4.1(http://www.umd.be/HSF/)(Béroud, 2010)"* (Hahn et al., 2019). The following selections were made: analyze a sequence and paste your own

sequence. *“The same sequence as mentioned above in part 1 was entered into the sequence box. The first and last nucleotide sections of the Ttn exon 335 were highlighted using nucleotide positions” (Hahn et al., 2019). Then “proceed to analysis now” was selected. “Upon viewing the generated ESE analysis, regions rich in ESEs closest to the above mentioned open/closed structures were noted.(3) The two best target sequence areas with the desired secondary structure regions and most enhanced ESEs were chosen. AONs, consisting of the reverse compliment of the target sequence, were constructed at a length of roughly 20 nucleotides long. (4)AON parameters were evaluated using the Oligo Calc tool (http://biotools.nubic.northwestern.edu/OligoCalc.html)(Kibbe, 2015). Areas at the beginning of the exon sequence with a maximum of 50 GC% were preferred; AON melting temperature greater than 48ºC was also favored, stretches of three or more Gs or Cs were avoided. (5) Energy values of the preliminary AONs were obtained using the RNAstructure bifold software (http://rna.urmc.rochester.edu/RNAstructureWeb/index.html)(Aligam, 2017). For calculating the AON free energy (ideal value >- 4), the AON sequence was entered into the sequence box and energy noted. For calculating the AON-AON interaction energy (ideal value > -15), the same AON sequence was entered into the two provided sequence boxes. For calculating the binding energy of the target and AON (ideal value 21-27), the binding energy of the target sequence and corresponding AON was subtracted from the free energy of the exon.(6) The initial AON sequences were checked for uniqueness (ideal value < 16 matches) using a nucleotide BLAST analysis (https://blast.ncbi.nlm.nih.gov/Blast.cgi).(7) The two AONs with most of the desired criteria met were then selected.(8) The AONs were synthesized and purified at Eurogentec, Germany. Each AON was chemically modified to gain exo- and endonuclease resistance through the addition of a 2’-O-methyl RNA group, with a full-length phosphorothioate backbone (Gramlich et al., 2015)”* (Hahn et al., 2019).

2.2 AON Transfection of HL-1 Cardiomyocytes

2.2.1 HL-1 Cell Culture

"The HL-1 mouse atrial cardiomyocyte tumor cell line was generously given to our to our lab from Dr. W. Claycomb, Departments of Biochemistry and Molecular Biology, Louisiana State University Medical Center, New Orleans. HL-1 cells were cultured using supplemented Claycomb medium(10% Fetal Bovine Serum, 0.1 mM Norepinephrine,2 mM L-Glutamine) and maintained as described(Claycomb et al., 1998)" (Hahn et al., 2019).

The following detailed steps were employed in the cell culture used in this study. The HL-1 cells were cultured in supplemented Claycomb medium. A T 175 flask was coated with 7ml coating medium at 37°C for at least 1 hour before seeding. Upon seeding the flask, coating medium was removed and 30ml of fresh supplemented medium added. Approximately 500µl of suspended HL-1 cells were added to flask. The flask was returned to a 37°C incubator for cell growth; medium was changed daily (Hahn et al., 2019).

Upon full cell confluency, confirmed by determining the cell population with a Zeiss microscope, cells were split. This was carried out by initially coating a new T175 flask with coating medium. Supplemented medium was removed from the flask and the confluent HL-1 cells were then rinsed twice with 25ml of PBS. 10ml of 0.05% Trypsin/EDTA was added to the flask and returned to the 37°C incubator for 10 minutes. Trypsinization was then stopped by adding 5ml of fresh, warmed supplemented medium. Cells were then transferred to a 15ml Falcon tube and centrifuged at 1200rpm for 5 minutes. Supernatant was removed and cells suspended in 4ml supplemented medium. The cells were then seeded into the new flask, approximately 250µl of cell solution was added (Hahn et al., 2019).

In order to freeze the HL-1 cells, cells were first trypsinized and centrifuged, supernatant was aspirated and cells were suspended in 2ml of freezing medium. The cells were transferred into cryovials (1 ml/vial) and the vials were placed in a freezing jar filled with room temperature isopropanol. The freezing

jar was placed into -80°C freezer immediately. One day after, the vials were moved to a -150°C freezer for long term storage (Hahn et al., 2019).

Supplemented Claycomb Medium:

10% FBS

0.1 mM Norepinephrine

2 mM L-Glutamine

Coating Medium:

0.005 mg/ml Fibronectin

0.02% Gelatin

Freezing Medium:

95% FBS

5% DMSO

2.2.2 HL-1 Cardiomyocyte Antisense Oligonucleotide Transfection

One day prior to the transient transfection, HL-1 cells were trypsinzed and seeded into a 6-well plate coated with the coating medium mentioned in section 2.2 and placed in the 37ºC incubator. Approximately 24h later, the cells were transfected with AONs. Samples were prepared as follows: AON1, AON2, AON1 and AON2 combined and control. AONs were prepared at a 200nM final concentration. Each sample was diluted with 200µL of 150mM NaCl solution in an Eppendorf tube; mixed by tapping the end of the tube for 10 seconds. PEI (Fermentas) transfection reagent was added to the salt and oligo sample mixtures at a ratio of 3.5 µl to 1 µg of AON and mixed again by tapping for 10 seconds. All samples were then set aside in room temperature to incubate for 10minutes. In the prepared 6-well plate, 200 µL of medium was removed from each well. Samples were added to corresponding wells; the plate was rocked by hand for 5 seconds and placed in the 37ºC incubator for 2 hours. Supplemented Claycomb medium as mentioned in section 2.2 was placed in each well and

returned to the 37ºC incubator for 24 hours; cells were then trypsinized and collected by centrifugation. RNA isolation followed (Hahn et al., 2019).

2.2.3 RNA Isolation of AON Transfected HL-1 Cells

Upon trypsinzation and collecting the transfected HL-1 cells by centrifugation, RNA was isolated using the RNeasy Mini Kit (Qiagen). After removing the supernatant, the cells were suspended in 350µl Buffer RLT and mixed by pipetting to dissolve the cell pellet. The cell mixture was placed in a QiaShredder column at 13,000rpm for 2minutes. In a 2ml collection tube the flow-through lysate was used for the further RNA isolation steps. 350 µl 70% ethanol was added to each sample and mixed by pipetting. The samples were then transferred to Qiaquick RNeasy spin columns and centrifuged for 15seconds at 8,600rpm, flow-through was discarded. The samples were then washed with 700 µl Buffer RW1 and centrifuged for 15seconds at 8,600rpm, flow-through was discarded. Next, samples were washed with 500 µl Buffer RPE and centrifuged for 15seconds at 8,600rpm, flow-through was discarded. 500 µl Buffer RPE was added to samples again and centrifuged for 2minutes at 8,600rpm, flow-through was discarded. For drying, columns were placed in a new collection tube and centrifuged for 1 minute at 13,000rpm. Caps of each sample were then opened and incubated at room temperature for 5minutes. Spin columns were then placed in sterile Eppendorf tubes; 30 µl of RNAse-free water was added to each sample and incubated at room temperature with caps closed for one minute. To elute RNA, samples were centrifuged at 8,600rpm for one minute. RNA was stored at -40ºC (Hahn et al., 2019).

2.2.4 cDNA Synthesis of AON Transfected HL-1 Cells

RNA samples were removed from the freezer and incubated at room temperature until thoroughly thawed. Total RNA concentration was measured using the Nanodrop (Therm Scientific). The cDNA was synthesized using reagents from the ImProm-II™ Reverse Transcription System (Promega) in a sterile, nuclease-free PCR tube, as followed: 1 µg of RNA, 2 µl mTTNEx320r primer and nuclease-free water, added to obtain a total volume of 5 µl. The

samples were mixed by pipetting and placed in a PCR instrument (Analytik Jena AG, Jena, Germany) for 5minutes at 70°C. Samples were then immediately placed on ice for 5minutes, then centrifuged for 10 seconds. The following was then added to each sample: ~4.5 µl nuclease-free water(adjusted to initial sample volume to reach total volume of 20 µl), 4 µl ImProm-II 5X Reaction Buffer, 4 µl $MgCl_2$, 1 µl dNTP Mix, 0.5 µl Recombinant RNasin Ribonuclease Inhibitor and 1 µl mProm-II™ Reverse Transcriptase. Samples were placed again in the PCR instrument as follows: 5 minutes at 25°C, 42°C for 1 hour and 70°C for 15 minutes (Hahn et al., 2019). Primer information is depicted in Table 2.

2.3 Nested RT-PCR

"In order to initially validate blocking Ttn exon 335 in the titin transcript, a nested RT-PCR was performed. Transfected cells were collected and RNA extraction was manually carried out using the RNeasy Mini Kit (Qiagen, Valencia, California, USA) according to the manufacturer's guidelines. The cDNA was synthesized using ImProm-II™ Reverse Transcription System (Promega, Mannheim, Germany) with the specific primer mTTNEx337r, according to the manufacturer's instructions. The two-round nested RT-PCR was established using the Expand Long Template PCR System (Roche)" per sample as follows Hahn et al., 2019). (1) First Round RT-PCR: 15.55µl PCR grade water, 1.5 µl $MgCl_2$, 5 µl buffer, 0.5 µl dNTPs, 0.6 µl mTTNEx333f, 0.6 µl mTTNEx337r, 0.25 µl DNA polymerase and 1 µl cDNA. The samples were placed in the PCR instrument with the following settings in the listed order: 5 minutes at 95°C, 20 cycles for 30 seconds at 25°C, 20 cycles for 30 seconds at 50°C, 20 cycles for 3.5 minutes at 72°C, 10 minutes at 72°C and 4°C for infinity. (2) Second Round RT-PCR per sample as follows: 15.55µl PCR grade water, 1.5 µl $MgCl_2$, 5 µl buffer, 0.5 µl dNTPs, 0.6 µl mTTNEx334f, 0.6 µl mTTNEx336r, 0.25 µl DNA polymerase and 1 µl First Round RT-PCR Product. The samples for PCR round two were placed in the PCR instrument with the following settings in the listed order: 5 minutes at 95°C, 35 cycles for 30 seconds at 25°C, 35 cycles for

30 seconds at 50°C, 35 cycles for 3minutes at 72°C, 1 minute at 72°C and 4°C for infinity…Agarose gel electrophoresis was performed following completion of the RT-PCR procedure. Semi-quantitive band intensity analysis was performed using the ImageJ Software (version ImageJ 1.x, Bethesda, MD); the gel analysis function was used to calculate percent difference between the wild type and skipped band. Primer sequence information is listed" in Table 2 (Hahn et al., 2019).

2.4 DNA Extraction and Sanger Sequencing

2.4.1 DNA Extraction and Sanger Sequencing Overview

"Further confirmation of blocking Ttn exon 335 in the transcript, without disruption of the reading frame, was achieved through direct Sanger sequencing. DNA extraction from the desired bands cut from the agarose gel was carried out using the QIAquick Gel Extraction Kit (Qiagen, Valencia, California, USA) according to the manufacturer's guidelines" (Hahn et al., 2019). DNA concentration was measured using Nanodrop (Therm Scientific).

The purified DNA samples were prepared at the concentration requested by the sequencing company (LGC Genomics Berlin, Germany) (Hahn et al., 2019). *"Samples were sequenced with the mTTNEx334f and mTTNEx336r primers"* (Hahn et al., 2019). The direct sequencing data was then analyzed and verified by comparing the nucleotide sequence data provided by the sequencing company and the known *Ttn* exon nucleotide sequences corresponding to the appropriate exons; the titin transcript reading frame was considered preserved when direct sequencing data showed the direct alignment of *Ttn* exon 334 followed by exon 336, without alteration (i.e. nucleotide addition or deletion) to normal sequence order. Primer sequence information is listed in Table 2 (Hahn et al., 2019).

2.4.2 Agarose Gel Electrophoresis

An agarose gel solution was prepared in a glass flask with 1.5g of agarose (SeaKem LE Agarose) added into 100ml 1x TAE buffer; the flask was then

placed in the microwave for 3 minutes. The heated solution was poured into an electrophoresis chamber with a comb in place. The gel solidified at room temperature for 30minutes; the comb was then removed, samples and 1kB marker were loaded into the gel. The electrophoresis took place for 45minutes at 140 Volts. The gel was stained with ethidium bromide for 10 minutes and imaged using a UV light; desired bands were cut out and stored in Eppendorf tubes at -4°C. Band intensity analysis was performed using the ImageJ software; the gel analysis function was used to calculate percent difference in bands (Hahn et al., 2019).

1x Tris-acetate-EDTA (TAE) Buffer:

40 mM Tris

20 mM acetic acid

1 mM EDTA, pH 8.4

2.4.3 DNA Extraction from Agarose Gel

The Qiagen QIAquick Gel Extraction kit was used to extract DNA from the agarose gel. The desired bands were cut out of the gel with a sterile scalpel and placed in labeled Eppendorf tubes. The samples were weighed and 3 volumes of Buffer QG was added to each sample. Incubation at 50ºC for 10minutes followed, samples were vortexed intermittently as needed to dissolve the gel in liquid. One gel volume of isopropanol was added to each sample, mixed by gently inverting the tubes. Samples were transferred to a QIAquick column and centrifuged at 13,000 rpm for 1 minute. The flow-through was discarded. Each column was washed with 500µl Buffer QG then with 750µl Buffer PE; centrifuged at 13,000rpm for 1 minute, each time discarding the flow-through. Columns were placed in a new collection tube and centrifuged again for 1minute at 13,000rpm. The columns were then placed in sterile Eppendorf tubes and incubated at room temperature with caps closed for 5minutes. For elution, 30µl of RNase-free water was added to the center of the membrane and incubated with the cap closed at room temperature for 1minute. Samples were then centrifuged at 13,000rpm for 1minute; eluted DNA was stored at -20ºC and

used for sequencing. DNA concentration levels were measured using the Nanodrop (Hahn et al., 2019).

2.4.4 Sanger Sequencing

The purified DNA samples were prepared at the concentration as requested by the sequencing company LGC Genomics Berlin, Germany. Samples were sequenced with the mTTNEx334f and mTTNEx336r primers (Table 2). The direct sequencing data was then analyzed by comparing the nucleotide sequence provided by the sequencing company and the known *Ttn* exon sequences of exon 334-336; the *titin* reading frame was considered preserved when direct sequencing data showed *titin* exon 334 and 336 conjoined, without alteration to the original exon sequences. To generate a graphical illustration of collected sequencing information, data was entered into MEGA7 software (version 7.0) (Hahn et al., 2019).

2.5 Calcium Measurements of AON Transfected HL-1 Cardiomyocytes

"To evaluate the cellular function of the AON transfected HL-1 cardiomyocytes, Store-Operated Calcium Entry (SOCE) measurements were performed" (Hahn et al., 2019). To prepare for the calcium measurements, "cells were transfected with AONs as previously mentioned in section 2.2.2" (Hahn et al., 2019). However, in each well a glass cover slide was initially placed in the well, followed by the coating medium. The calcium measurements were performed approximately 24 hours after transfection completion" by Dr.rer.nat. Lisann Pelzl at the University Of Tübingen, Physiology Department (Hahn et al., 2019).

"In order to conduct the calcium measurements, Fura-2/AM fluorescence was utilized to determine cytosolic Ca2+ concentration ([Ca2+]i) as previously described(Al-Maghout et al., 2017). The cells were loaded with Fura-2/AM (2 μM, Invitrogen, Goettingen, Germany) for 15 minutes at 37°C. Cells were then excited alternatively at 340 nm and 380 nm through an objective (Fluor 40×/1.30

oil) built in an inverted phase-contrast microscope (Axiovert 100, Zeiss, Oberkochen, Germany). Emitted fluorescence intensity was recorded at 505 nm. The data was acquired using specialized computer software (Metafluor, Universal Imaging, Downingtown, USA). The cytosolic Ca2+ activity was estimated from the 340 nm/380 nm ratio. Store-Operated Calcium Entry was determined by extracellular Ca2+ removal and subsequent Ca2+ re-addition in the presence of thapsigargin (1 µM, Invitrogen). For quantification of Ca2+ entry, the slope (delta ratio/s) and peak (delta ratio) were calculated following re-addition of Ca2+. Experiments were performed with Ringer solution containing (in mM): 125 NaCl, 5 KCl, 1.2 MgSO4, 2 CaCl2, 2 Na2HPO4, 32 HEPES, 5 glucose, pH 7.4. To reach nominally Ca2+-free conditions, experiments were performed using Ca2+-free Ringer solution containing (in mM): 125 NaCl, 5 KCl, 1.2 MgSO4, 2 Na2HPO4, 32 HEPES, 0.5 EGTA, 5 glucose, pH 7.4(Al-Maghout et al., 2017)" (Hahn et al., 2019).

2.6 Immunofluorescent Imaging and Analysis of AON Transfected HL-1 Cardiomyocytes

"To assess the organization of sarcomeric proteins in the transfected HL-1 cells, immunofluorescent imagining was performed" (Hahn et al., 2019). For immunofluorescent staining, cells were transfected with AONs as previously mentioned in section 2.2.2 of this paper. However, in each well a cover glass was initially placed, followed by addition of the coating medium. Upon completion of transfection, 4% (vol/vol) paraformaldehyde was added to each well and incubated at room temperature for 10 minutes. Permeabilization solution (1ml) was then added to each well and incubated at room temperature for 10 minutes. Blocking solution (200µl/well) was added and incubated at room temperature for 30minutes. The following primary antibodies were added to appropriate wells and incubated overnight at 4ºC: Anti-Sarcomeric Alpha-Actinin (1:200) and Anti-Titin (1:50). On the following day, primary antibodies were removed. The wells were washed with PBS three times for 5 minutes each at room temperature, on a slow-moving rocking plate. The following secondary

antibodies were added to each well and incubated in darkness at room temperature for 1 hour: Goat Anti-Rabbit Alexa Fluor 555(1:200) and Goat Anti-Mouse Alexa Fluor 488(1:200). The wells were then washed again with PBS three times for 5 minutes each at room temperature on a slow-moving rocking plate. At a dilution of 1:3000 in PBS, DAPI was added to each well and incubated in darkness for 3 minutes. Wells were washed again with PBS one time for 2 minutes. Fluorescent Mounting Medium (Dako) was used to mount the cover slides; samples dried overnight at room temperature and were then stored at 4ºC for further storage" (Hahn et al., 2019).

"Imagery was performed using a Zeiss fluorescent microscope. In total, 200 cells from each sample group were randomly chosen for image analysis; each evaluated cell was categorized as "fully organized" or "partially organized" based upon the overall order of alpha-actinin and titin striations throughout the entire cytoplasm of considered cells" (Hahn et al., 2019).

Antibodies:

Anti-Sarcomeric Alpha-Actinin (EA-53,mouse, Abcam)
Anti-Titin (ab193218,rabbit, Abcam)
Goat Anti-Rabbit, Alexa Fluor 555(Invitrogen)
Goat Anti-Mouse, Alexa Fluor 488 (Invitrogen)

Antibody Dilution Solution:

1% BSA in PBS

Permeabilization Solution:

0.1% Triton X-100 in PBS

Blocking Solution:

10% Goat Serum in PBS

2.7 Cell Fractional Shortening of AON Transfected HL-1 Cardiomyocytes

"To determine the transfected cell fractional shortening, video assisted planimetry was conducted. Contracting HL-1 cells were transiently transfected," as mentioned in section 2.2.2 of this paper (Hahn et al., 2019). *"Cell recording was performed approximately 24 hours after transfection completion. HL-1 cell contraction was recorded with a microscope connected to a video camera; the video was saved on disc using a DVD player. In total, 20 beating cells were chosen at random for each sample group. For each cell, 10 continuous beats were recorded and used for further measurement. Video material was extracted at 2 frames per second (2fps) for 10 seconds using the VirtualDub program (version 1.10.4). The largest and smallest area of each cell was measured in its corresponding 20 picture frames using the Gimp program (version 2.10.6); images were measured at a 300% zoom setting. Data was collected from two separate cell preparations and entered into the Microsoft Excel program"* (Hahn et al., 2019). *"Averaged largest (end diastolic volume) and smallest (end systolic volume) area for each cell was calculated for determining cell fractional shortening;" th*e square root of the change in the area was calculated (Hahn et al., 2019). *"The following formula was used for cell fractional shortening (%) calculation: square root of: [(end diastolic volume - end systolic volume)/ (end diastolic volume)]*100"* (Hahn et al., 2019).

3. Results

3.1 Design of AONs

"In this study we designed AON1 and AON2 to block the exonic splicing enhancer motifs of Ttn exon 335 in the HL-1 cell line as illustrated in our study schema (Figures 1.1, 1.2, 1.3). The AONs were further chemically modified to gain exo- and endonuclease resistance through the addition of a 2'-O-methyl RNA phosphorothioate backbone(Gramlich et al., 2015)" (Hahn et al., 2019).

We identified the corresponding mouse exon sequence which resembled our target human TTN exon by using the Ensemble website (Zerbino et al., 2018). For this process, we compared the TTN exon 335 human sequence (Figure 2.1) to the *Ttn* mouse exon sequence data. We found the mouse *Ttn* exon 318 best resembled TTN 335, as seen in Figure 2.2(for the purpose of simplicity, we refer to the mouse exon *Ttn* 318 as *Ttn 335* and adapt the preceding *Ttn* intron 317 as *Ttn* intron 334 accordingly). Although the two sequences were not exact, similarity between the intron and exon sequences was confirmed by matching end flanking intron sequences and by finding high similarity in the beginning and end portions of the exons as illustrated in the underlined portions of Figures 2.1 and 2.2. For the software used for AON design (section 2.1) a select portion of the mouse intron/exon sequence was used as seen in Figure 2.3 (Hahn et al., 2019).

"In the design process, the complete secondary structure of Ttn exon 335 was generated and analyzed, including the last 50nt of the flanking Ttn intron 334" and the initial 150 nucleotides of *Ttn* exon 335 (Hahn et al., 2019). The portion of the nucleotide sequence used for AON design is depicted in Figure 2.3, as only a limited number of nucleotides were able to be entered into the software used (Hahn et al., 2019). A complete and "*partial view of the secondary structure with suitable target regions of the exon for AON design are depicted*" in Figure 2.4 and 2.5 (Hahn et al., 2019). *"Target regions display both partially*

open and closed structures, located specifically at Ttn exon 335 nucleotide numbers 1-20 and 50-70. Upon ESE analysis, these precise regions of the exon also proved to be enhanced with ESEs, shown in Figure 2.6. Combining these results along with considering the GC% and melting temperature of each potential AON sequence, we chose these two regions as our target sequences for AON design. The generated AON sequences of AON1 and AON2 as well as the free energy calculations are shown in Table 1" (Hahn et al., 2019). We could not explain the "no pairs" result in calculating AON free energy; this was noted and the AON2 was chosen overall suitable for testing despite this parameter result (Hahn et al, 2019). *"Overall, both AONs met most of the AON design criteria mentioned previously in section 2.1 of this paper"* (Hahn et al., 2019).

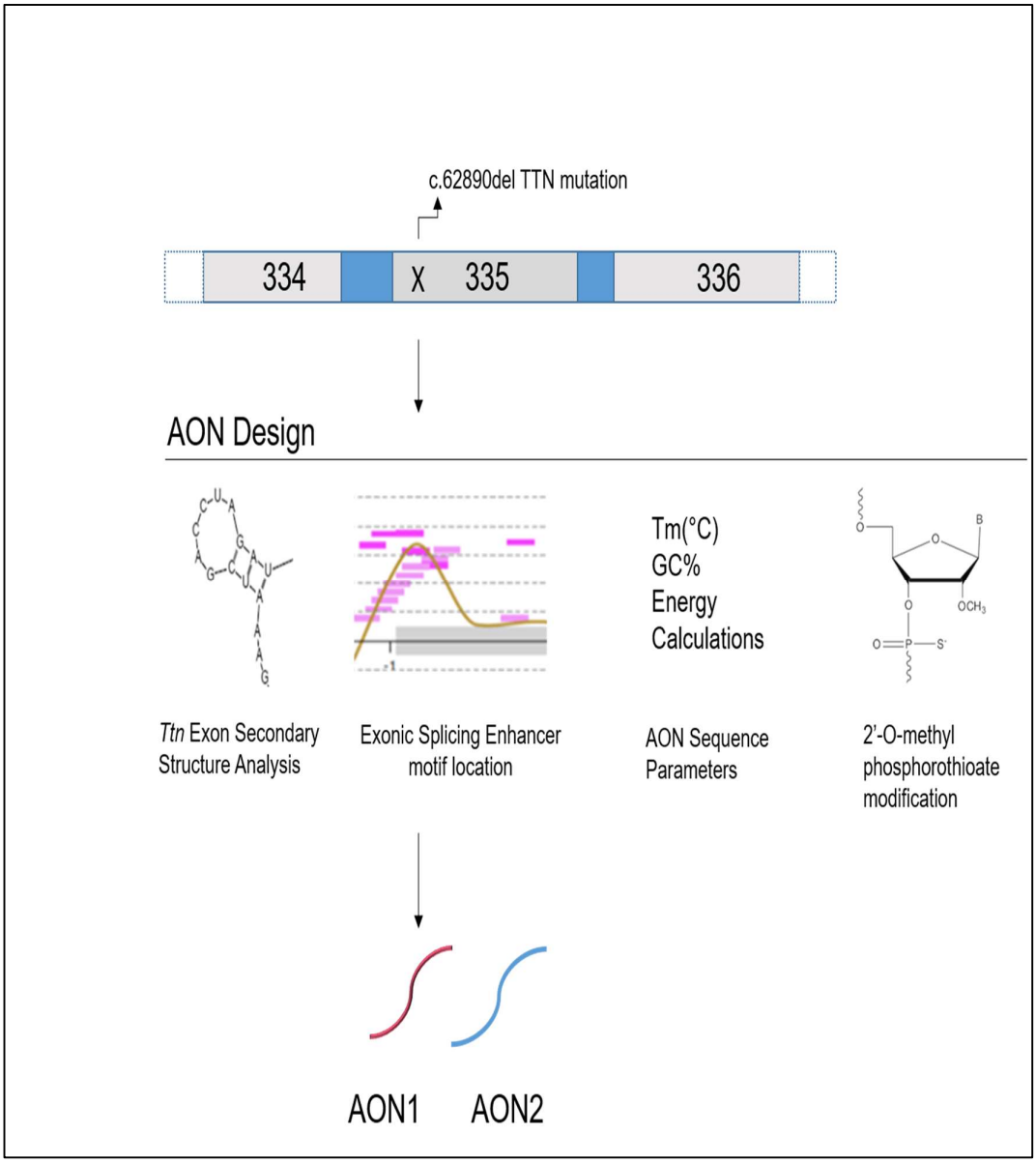

Figure 1.1: Study Schematic, AON Design for Titin Mutation
"Schematic of study layout," (Hahn et al., 2019). Depiction of initial step of this study: identification of the TTN mutation related to DCM, here seen as TTN exon 335. The following steps for AON-mediated exon skipping for this particular exon include: identification of the mouse species mutation, generation of secondary structure prediction with notation of open and closed structures, ESE motif location, AON parameter calculations(Aartsma-Rus, 2012) and proper chemistry determination(Hahn et al., 2019). **This figure was originally published as seen in Hahn et al., 2019.*

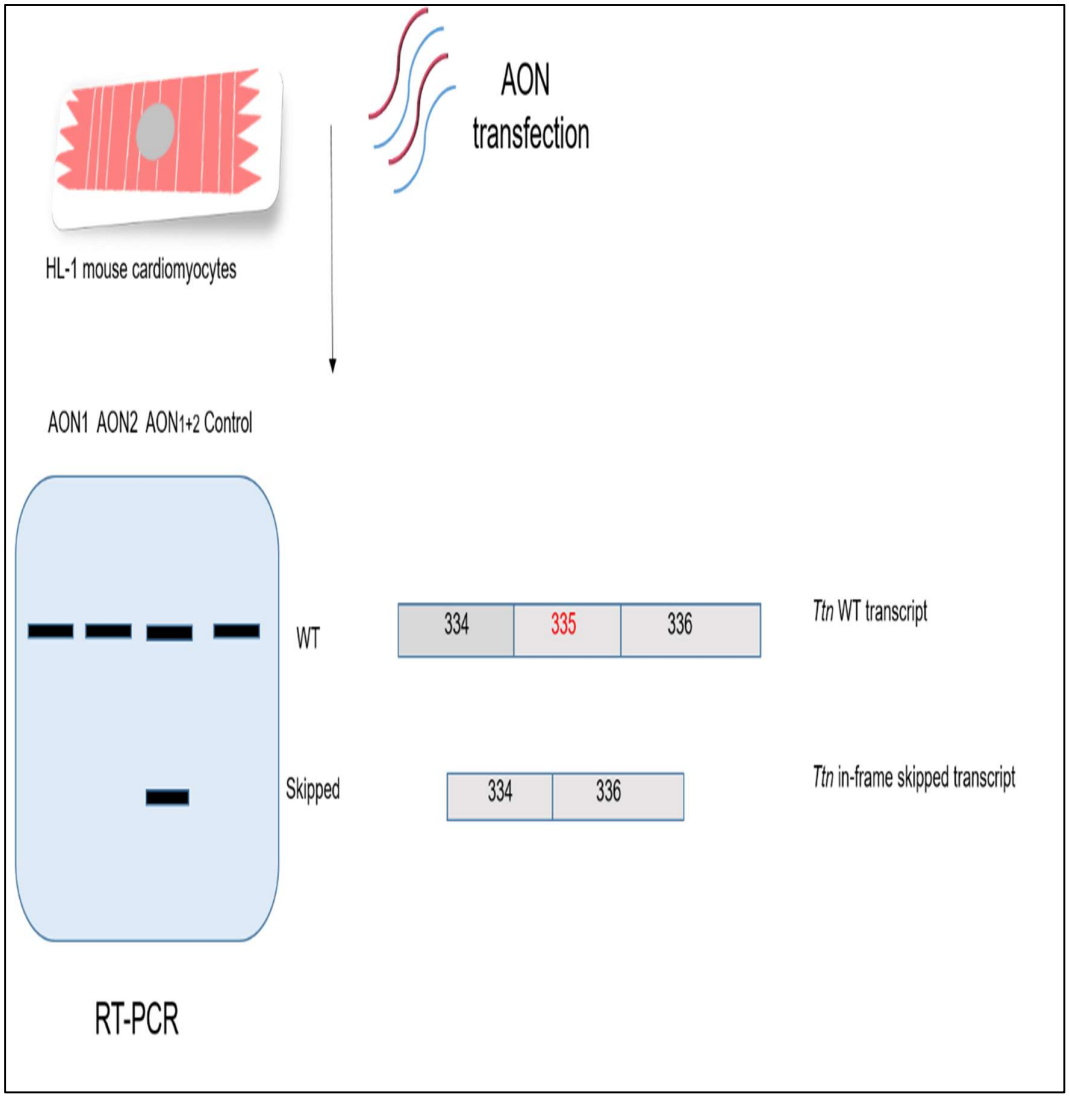

Figure 1.2: Study Schematic, Validation of *Ttn* Exon Skipping
Illustration of transient AON transfection with specific AON designed for *Ttn* exon 335. Upon transfection completion, RT-PCR and Sanger sequencing were completed to confirm exon skipping (Hahn et al., 2019).

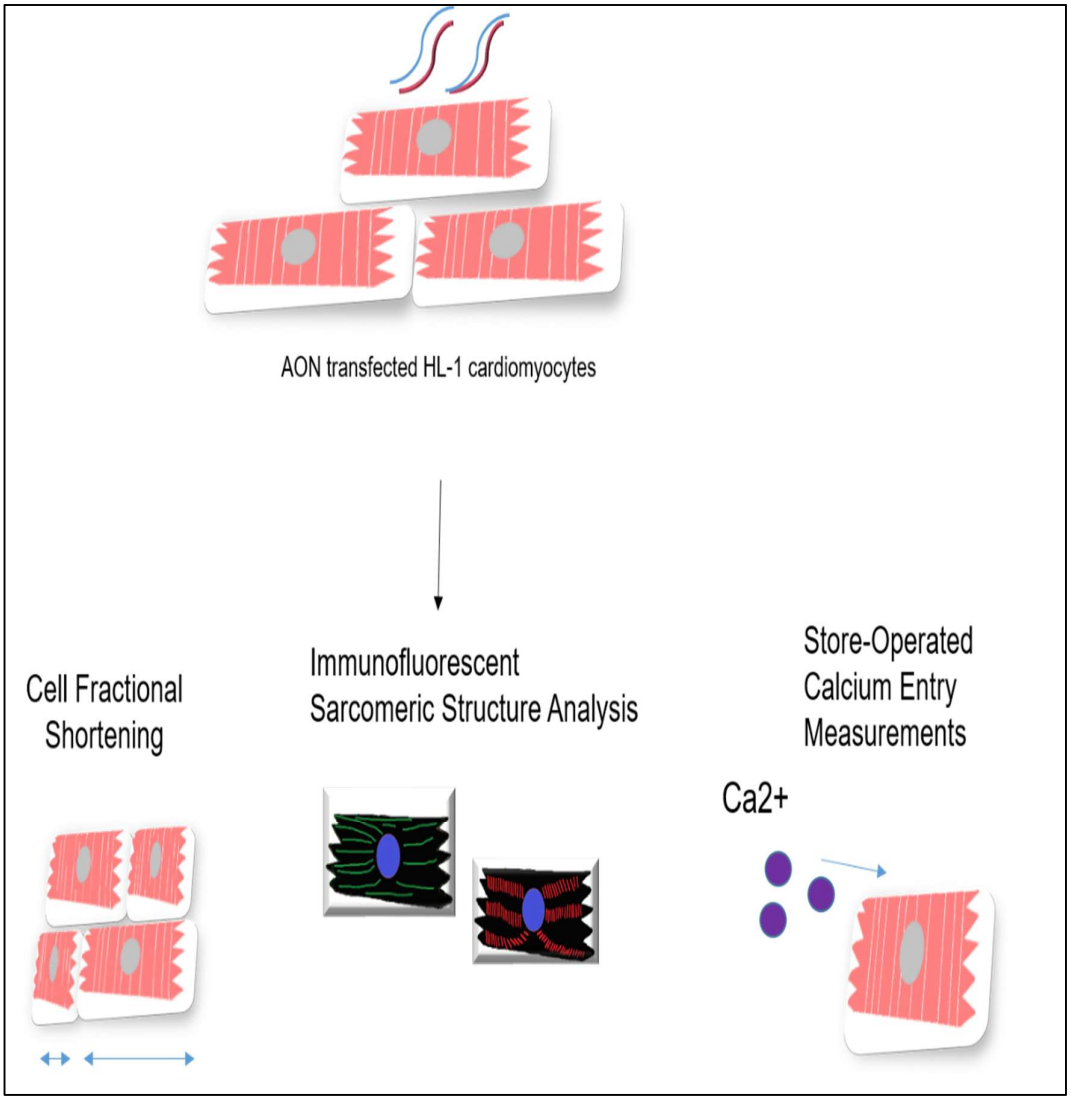

Figure 1.3: Study Schematic, Evaluation of AON Transfected HL-1 Cells
Illustration of dynamic set of experiments for evaluation of cell vitality and functionality upon blocking the target exon (Hahn et al., 2019).

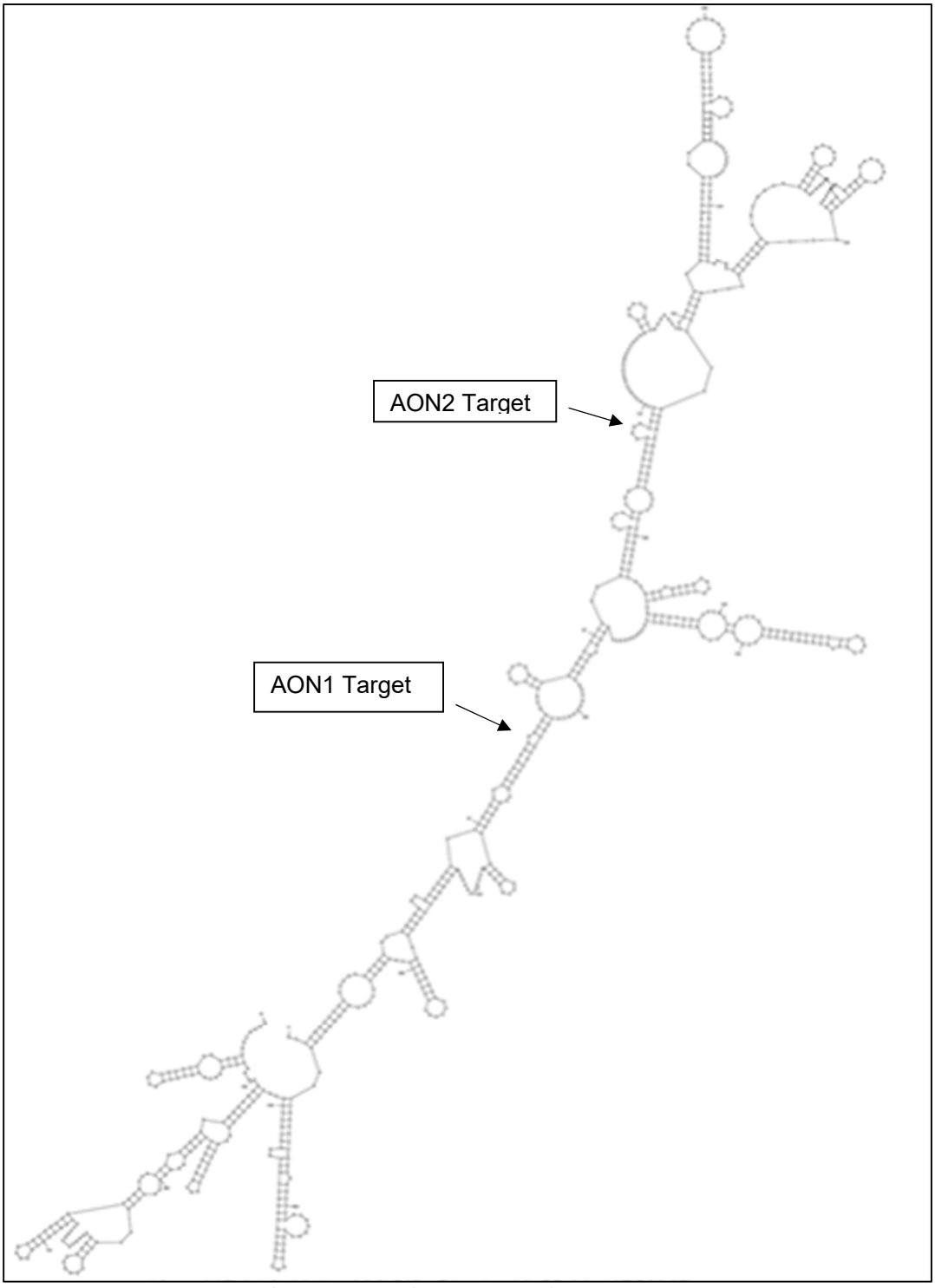

Figure 2.4 Predicted Secondary Structure of *Ttn* Exon 335
Predicted secondary structure constructed using the RNAstructure Web Server(Aligam, 2017); structure includes flanking 50 nucleotides of *Ttn* intron 334 and the first 150 nucleotides of *Ttn* exon 335 as seen in Figure 2.1(Hahn et al., 2019).

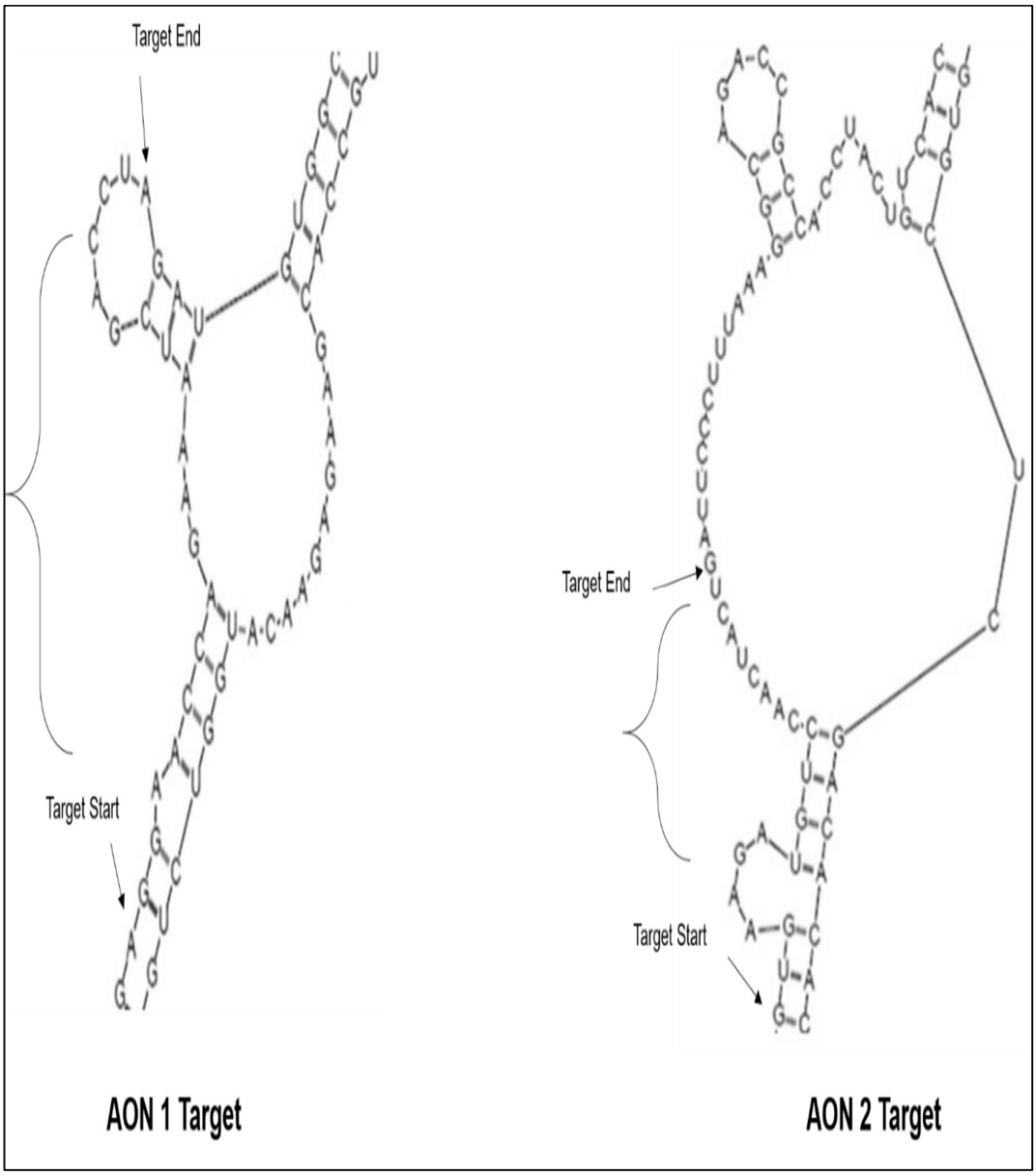

Figure 2.5: Antisense Oligonucleotide Design for *Ttn* exon 335, Target Zones

"Secondary structure prediction of Ttn exon 335 using RNAstructure(Aligam, 2017)*"* as seen in Figure 2.4 (Hahn et al, 2019). *"Two separate sections of the secondary structure are illustrated to depict AON1 and AON2 target zones. Brackets indicate areas of desired partially open and closed structures for target sequence selection. Selected target zones are marked with black arrows"* (Hahn et al., 2019). **This figure was originally published as seen in Hahn et al., 2019.*

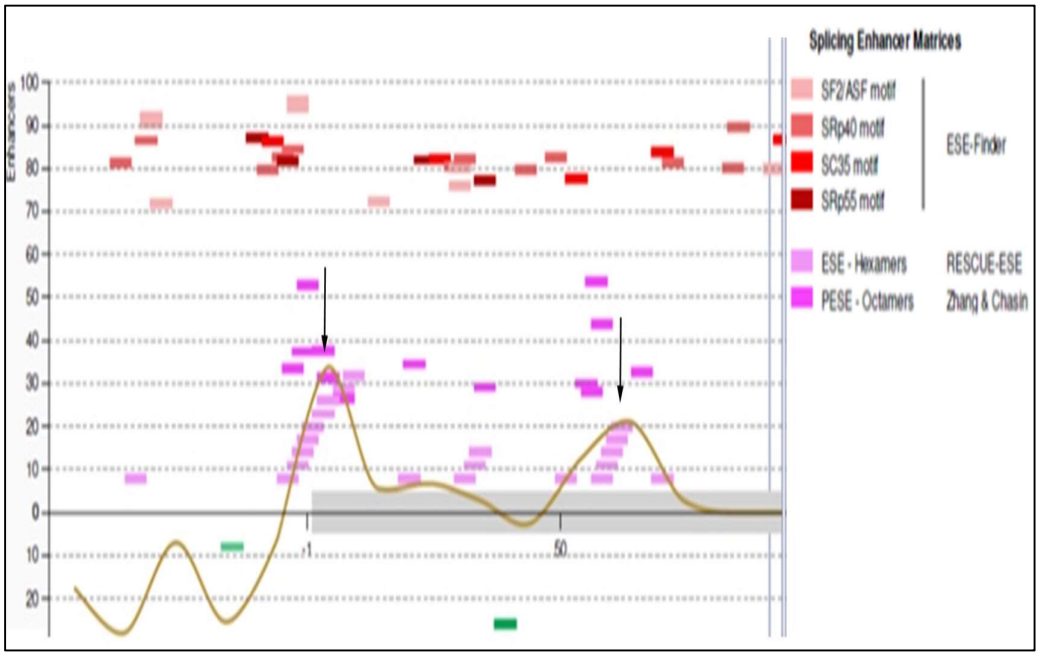

Figure 2.6: Antisense Oligonucleotide Design for *Ttn* exon 335, ESEs
"Predicted location of exonic splicing enhancer motifs (ESEs) of Ttn exon 335 using Human Splicing Finder 2.4 (Béroud, 2010). ESEs are marked by the light pink bars; the grey bar represents the first 150nt of the exon. Enhanced regions of ESEs are marked with black downward arrows. The two AON target sequences were chosen in these regions" (Hahn et al., 2019). **This figure was originally published as seen in Hahn et al., 2019.*

Table 1: AON Design Parameters
AON parameter criteria listed for AON1 and AON2, provided with reference values as previously published(Aartsma-Rus, 2012). Energy calculations made from RNAstructure bifold software (Aligam, 2017); melting temperature and GC% calculated from online webserver Oligo Calc tool(Kibbe, 2015)(Hahn et al., 2019). **This table was originally published as seen in Hahn et al., 2019.*

AON	Target Sequence	AON Sequence	Tm(°C)	GC%	AON Free Energy	AON-AON Interaction Energy	Binding Energy of Target and AON	Blast Analysis Nucleotide Match
Reference Values		~ 20nt	> 48	40-50	< -4	< -15	21-27	< 15
AON1	AGGAACCA GAAATCGA CCTA	UAGGUCGAUUUCU GGUUCCU	50	45	-0.5	-8.1	27.3	13
AON2	GTGAAGAT GTCCAACTA CTG	CAGUAGUUGGACA UCUUCAC	50	45	No pairs	-7	30.2	15

3.2 Confirmation of AON-mediated skipping of *Ttn* exon 335 in HL-1 Cardiomyocytes

"We confirmed AON-mediated blocking of Ttn exon 335 in the titin transcript from AON treated HL-1 cells by utilizing a nested RT-PCR and direct sequencing" (Hahn et al., 2019). A list of the primers used for this process is illustrated in Table 2. *"Depicted in Figure 3.1, our results demonstrate only transiently transfected HL-1 cells with the combination of both AON1 and AON2 successfully prevent the integration of Ttn exon 335 in the titin transcript without disrupting the sequence of the natural reading frame. This is shown in the*

presence of the representative "skipped" band at 600bp in the sample AON1+AON2 which is indicative of the molecular weight of the conjoined transcript containing Ttn exons 334 and 336. In direct sequencing of the skipped band at 600bp, preservation of both nucleotide sequences of Ttn exons 334 and 336 were observed. The sequence data (Figure 3.2) *of Ttn exon 334 conjoined to the nucleotide sequence of Ttn exon 336 without deletion or inclusion of other nucleotides, shows a conserved reading frame with the omission of the target Ttn exon 335 transcript. Based on ImageJ band intensity analysis* (Figure 3.3) *between the Ttn wildtype band representative of the Ttn exon 334, 335 and 336 transcript and the skipped band representative of the Ttn exon 334 and 336 transcript, it is estimated that approximately 76% of the wildtype transcript was successfully skipped and contributed to the band intensity found in the 600bp skipped band. Transfected cells with only AON1 or only AON2 showed no evidence of blocking the Ttn exon 335 transcript, indicated in our RT-PCR results by the absence of the skipped band at 600bp. In addition, all samples depict a wildtype band at the 2,000bp marker"* (Hahn et al., 2019).

Table 2: Primers for nested RT-PCR, cDNA and direct Sanger sequencing (Hahn et al., 2019).

Name	**Species**	**Sequence**
mTTNEx333f	Mouse	TAGCCAAGAATGCCTTTGTTACACCTG
mTTNEx337r	Mouse	TGGCCCGACTACTTTTCCTGGTGTATC
mTTNEx334f	Mouse	GCTGCTGATCCAATTGATCCTCCAG
mTTNEx336r	Mouse	CTGTTGGTGGAACGTTTTCATCTCTTG

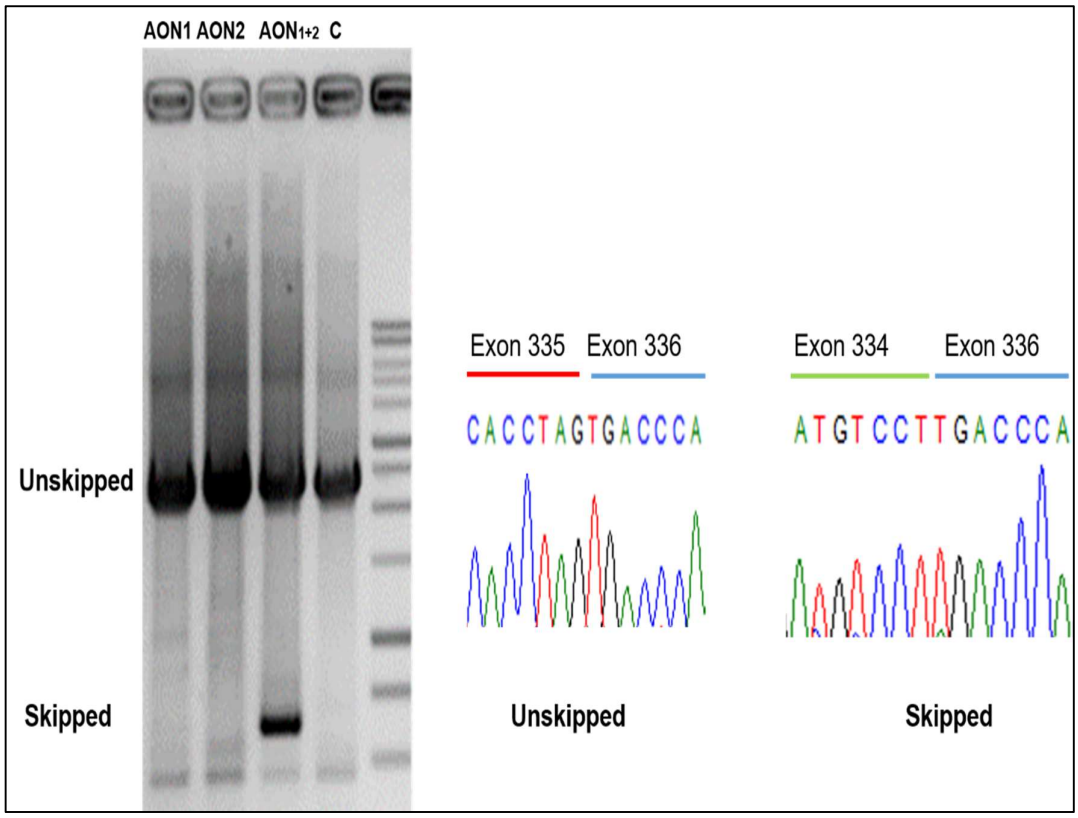

Figure 3.1: Exon Skipping Validation in AON Transfected HL-1 Cells
"Exon skipping scheme and validation of antisense oligonucleotides in HL-1 mouse cardiomyocytes. RT-PCR analysis (left) and representative direct sanger sequencing (right) of Ttn exon 335" (Hahn et al., 2019). Samples depicted: AON1, AON2, AON1+AON2, and Control(C) transfected HL-1 cardiomyocytes. **This figure was originally published as seen in Hahn et al., 2019.*

(A)Sequencing Results:

***Ttn* Exon 334 /Ttn Exon 336**

GCAGACTCGACCAAATCATCCATCACCCTTGGCTGGAGTAAGCCTGTCT
ATGATGGTGGCAGTGATGTTACTGGATATGTGGTTGAGATGAAACAAGG
AGATGAAGAAGAATGGACCATTGTCTCTACCAGGGGAGAGGTCAGAAC
TACAGAATATGTGGTCTCTAACCTGAAACCCGGAGTCAATTATTATTTCC
AAGTATCAGCAGTAAACTGTGCCGGCCAAGGAGAACCTATAACAATGAC
TGAACCTGCACAGGCTAAAGATGT**CCTTG****ACCCA**CCCGGCACTCCTGA
CTACATTGATGTCACCCGGGAAACCATCACACTTAAATGGAACCCACCA
TTACGTGATGGGGGCAGTAAGATCGTGGCCTACAGCATTGAGAAGCGG
CAAGGAAGTGACCGCTGGGTGAGATGCAACTTCACTGACGTCAGTGAG
TGTCAGTACACAGTTACGGGACTCAGTCCTGGAGATCGATATGAGTTCA
GAATAATTGCAAGAAATGCTGTTGGCACTATAAGCCCCCCCTCACAGTC
TTCTGGCCTCATTATGACAAGAGATGAAAACG

(B) Published *Ttn* Exon Sequences

***Ttn* Exon 334:**

ATCCTCCAGGACCACCTGCCAAGATAAGAATTGCAGACTCGACCAAATC
ATCCATCACCCTTGGCTGGAGTAAGCCTGTCTATGATGGTGGCAGTGAT
GTTACTGGATATGTGGTTGAGATGAAACAAGGAGATGAAGAAGAATGGA
CCATTGTCTCTACCAGGGGAGAGGTCAGAACTACAGAATATGTGGTCTC
TAACCTGAAACCCGGAGTCAATTATTATTTCCAAGTATCAGCAGTAAACT
GTGCCGGCCAAGGAGAACCTATAACAATGACTGAACCTGCACAGGCTA
AAGATGT**CCTTG**

***Ttn* Exon 336:**

ACCCACCCGGCACTCCTGACTACATTGATGTCACCCGGGAAACCATCA
CACTTAAATGGAACCCACCATTACGTGATGGGGGCAGTAAGATCGTGG
CCTACAGCATTGAGAAGCGGCAAGGAAGTGACCGCTGGGTGAGATGCA
ACTTCACTGACGTCAGTGAGTGTCAGTACACAGTTACGGGACTCAGTCC
TGGAGATCGATATGAGTTCAGAATAATTGCAAGAAATGCTGTTGGCACT
ATAAGCCCCCCCTCACAGTCTTCTGGCCTCATTATGACAAGAGATGAAA
ACG

Figure 3.2: Sanger Sequencing Data of "Skipped band" from AON1+2 Transfected HL-1 Cells with Known Corresponding Exon Sequences for Comparison

The illustrated sequence **(A)** is a sample of our Sanger sequencing data of the purified DNA sample gathered from the "Skipped band" at 600bp marker as seen in Figure 3.1 All sequencing was performed at LGC Genomics(Berlin, Germany) with our specific mTTNEx334f primer(Table 2) . **(B)**The corresponding *Ttn* exon 334(grey) and 336(black) exon sequences (Ensembl, release verision 93) are featured for sequence comparison for a detailed illustration of verifying the *Ttn* transcript remained preserved while blocking the *Ttn* exon 335 from the transcript(Zerbino et al., 2018). Underlined sections indicate matching exon portions (Hahn et al., 2019).

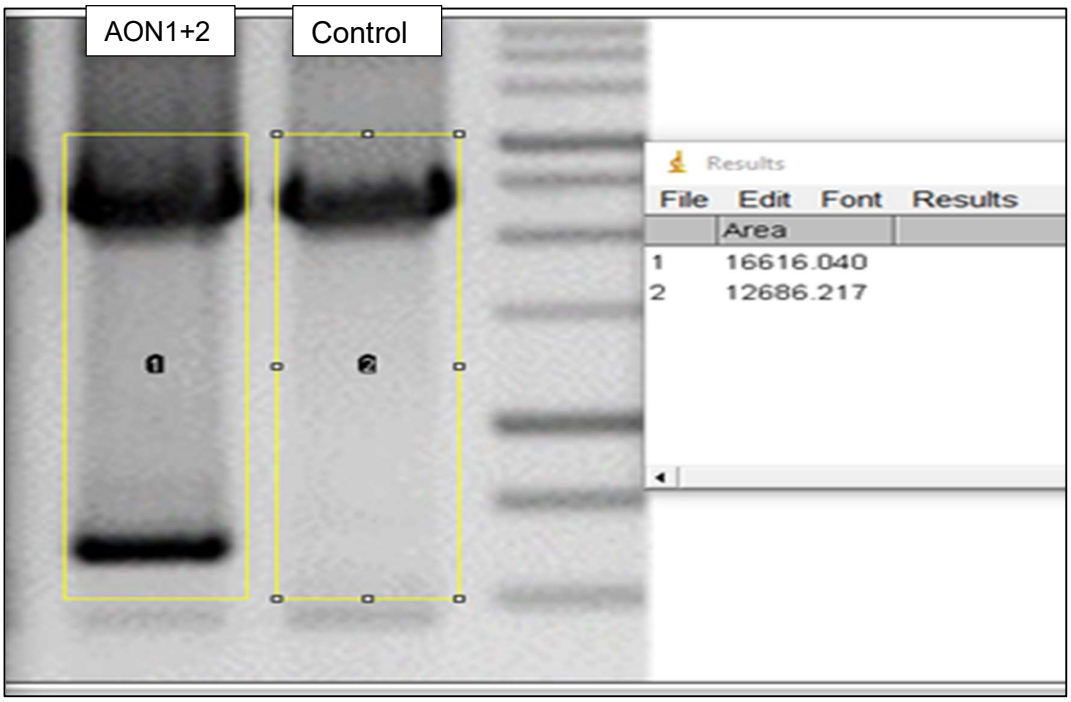

Figure 3.3: Band Intensity Analysis of "Skipped band" and Unskipped band (wild type) of AON Transfected HL-1 Cells

Band Image analysis results using ImageJ software in order to provide an approximation of the amount of the wild type transcript successfully exon skipped by the combination of AON1+2. As seen in Figure 3.1, RT-PCR Image with magnification on area of interest. Calculation as follows: Approximation in percent, from pixel measurements depicted of comparing bands in (1)= AON1+2 sample,(2)=Control sample in selection of image outlined: ((12686.217/16616.04)*100)= ~76%) (Hahn et al., 2019).

3.3 Assessment of AON transfected HL-1 Cardiomyocytes

"We further assessed the impact of AON treatment in HL-1 cardiomyocytes on the following: organization of sarcomeric protein striations through immunofluorescent imagery, store-operated calcium entry activity and cell fractional shortening through video-assisted planimetry" (Hahn et al., 2019).

3.3.1 Immunofluorescent imagery of AON transfected HL-1 cells

"In order to analyze the sarcomeric structures of the AON-treated HL-1 cardiomyocytes, we enhanced the Z-disk proteins alpha-actinin and titin with immunofluorescent microscopy. Results were obtained by categorizing 200 randomly chosen cells as "fully organized" or "partially organized" for each sample group AON1+2 and control. We designated cells as "fully organized" when alpha-actinin and titin structures formed orderly striations throughout most of the cardiomyocyte cytoplasm as shown in Figure 4. "Partially organized" cells displayed lesser or poorly ordered striations throughout the entire cell cytoplasm, compared to fully organized cells. The chi-squared test was used to determine significant differences in the level of sarcomere organization between sample groups for alpha-actinin and titin immunofluorescent images. No significant differences in the level of sarcomeric organization were observed in comparing samples groups AON1+2 transfected HL-1 cells (n=200) and control (n=200) (Figure 5)*"* (Hahn et al., 2019). Statistical tests were performed using the software GraphPad Prism (version 7.05). A difference was considered significant when $P<0.05$.

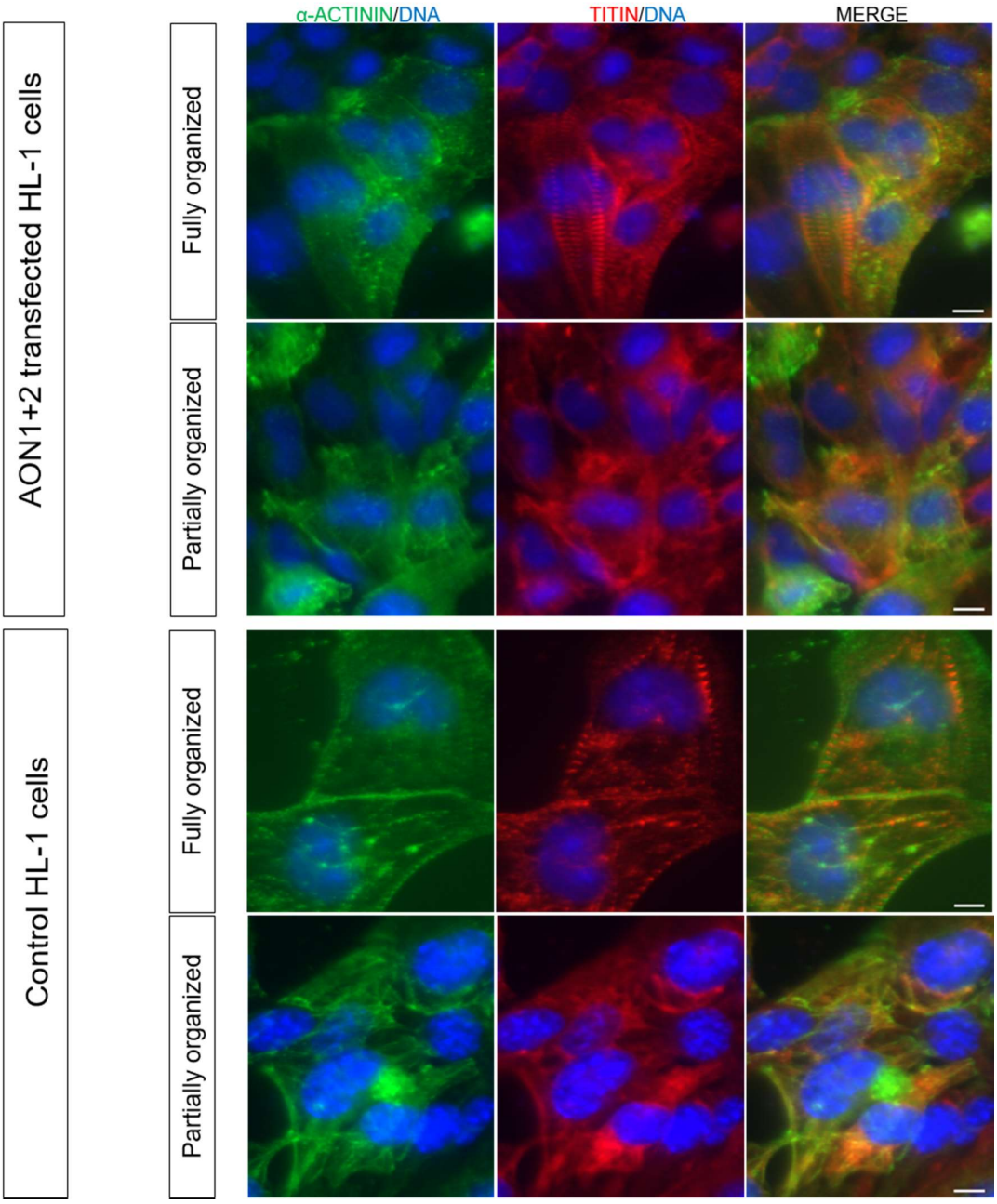

Figure 4: Sarcomeric Protein Immunofluorescent Imagery
"Sarcomeric protein immunofluorescent microscopy of AON transfected HL-1 cardiomyocytes. Fluorescence images illustrating fully and partially organized sarcomeric proteins alpha-actinin (green) and titin (red) in randomly selected AON1+2 transfected HL-1 cardiomyocytes and in control group cells. Cell categorization of AON1+2 transfected HL-1 cells (n=200) and control (n=200). Scale bars, 5 µm" (Hahn et al., 2019). **This figure was originally published as seen in Hahn et al., 2019.*

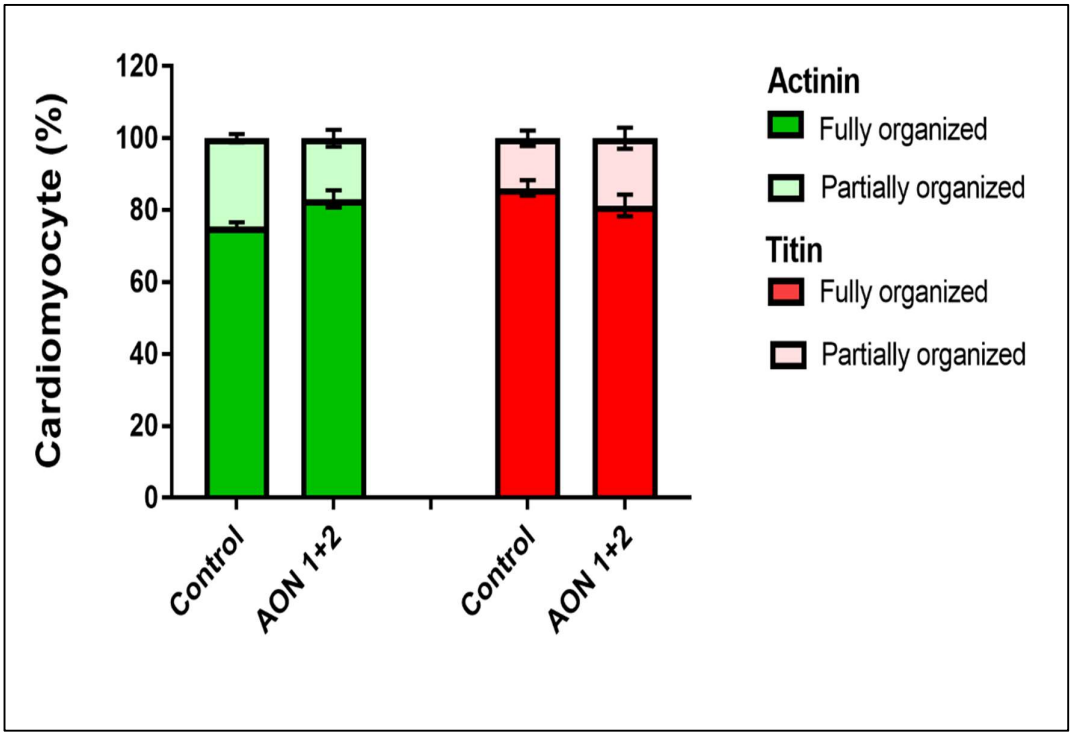

Figure 5: Sarcomeric Protein Immunofluorescent Imagery Analysis of AON Transfected HL-1 Cardiomyocytes

"Image analysis, calculation based on cell categorization (Figure 4) of AON1+2 transfected HL-1 cells (n=200) and control (n=200). Percentage of cardiomyocyte with corresponding organizational level depicted. Statistical difference was tested using the chi-squared test. No significant differences were observed comparing level of sarcomeric organization between groups in alpha-actinin and in titin analyzed images. Data represent mean values ± SEM" (Hahn et al., 2019). **This figure was originally published as seen in Hahn et al., 2019.*

3.3.2 Calcium Measurements of AON transfected HL-1 cells

"To further evaluate essential molecular function in AON treated HL-1 cells, we performed calcium cell measurements. In four separate preparations of AON1+2 transfected HL-1 cells and control groups, we determined the Store-Operated Calcium Entry (SOCE) of the cells. In these experiments, as illustrated in Figure 6, we observed a similar trend in the representative increase of cytosolic Ca^{2+} activity, between AON1+2 and control Fura-2/AM loaded samples, initiated by exposure to Ca^{2+}-free solution, then triggered by subsequent additional exposure to thapsigargin(a well-established inhibitor of sarcoendoplasmatic reticulum Ca^{2+} ATPase) and re-addition of extracellular Ca^{2+}. The slope (delta ratio per second) and peak (delta ratio) of the fluorescence ratio changes following re-addition of extracellular Ca^{2+} in both samples groups were calculated (Figures 7 and 8). Using the two-sided Student's t-test to determine statistical difference between samples, in both slope and peak calculations, there were no significant differences between AON1+2 transfected HL-1 cells and control cells observed (n=56-60 cells)" (Hahn et al., 2019). Statistical tests were performed using the software GraphPad Prism (version 7.05). A difference was considered significant when $P<0.05$.

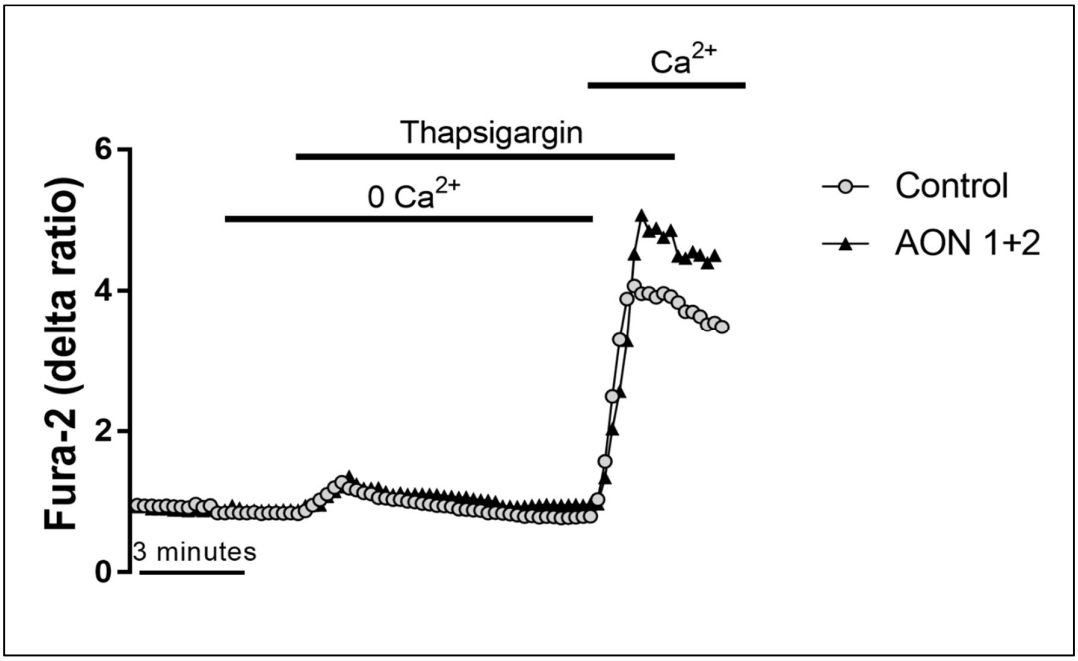

Figure 6: SOCE in AON Transfected HL-1 Cells

"Store-operated Calcium Entry (SOCE) calculated by representative tracings showing the 340/380 nm fluorescence ratio reflecting cytosolic Ca^{2+} activity in Fura-2/AM loaded samples of AON1+2 transfected HL-1 cells and control following exposure to Ca^{2+}-free HEPES, additional exposure to thapsigargin (1μM) and re-addition of extracellular Ca^{2+}. Results are summarized from 56–60 cells from four different preparations" (Hahn et al., 2019). **This figure was originally published as seen in Hahn et al., 2019.*

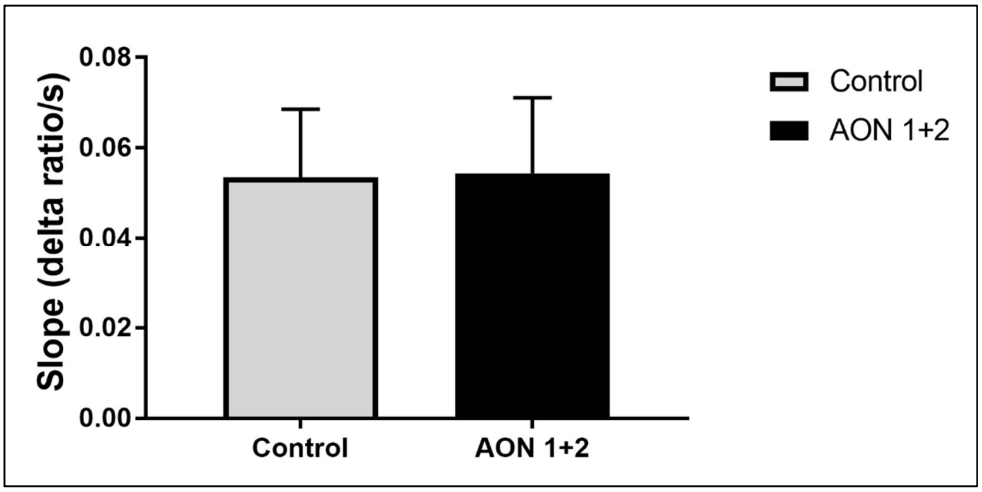

Figure 7: SOCE in AON Transfected HL-1 Cells, Slope (delta ratio/s) Arithmetic means ± SEM (n =56–60 cells) of the slope of the fluorescence ratio change seen in Figure 6 following re-addition of extracellular Ca^{2+} in AON1+2 transfected HL-1 cells (black bar) and control (grey bar). Statistical difference was tested using the two-sided Student's t-test. No significant differences were observed between groups (Hahn et al., 2019). **This figure was originally published as seen in Hahn et al., 2019.*

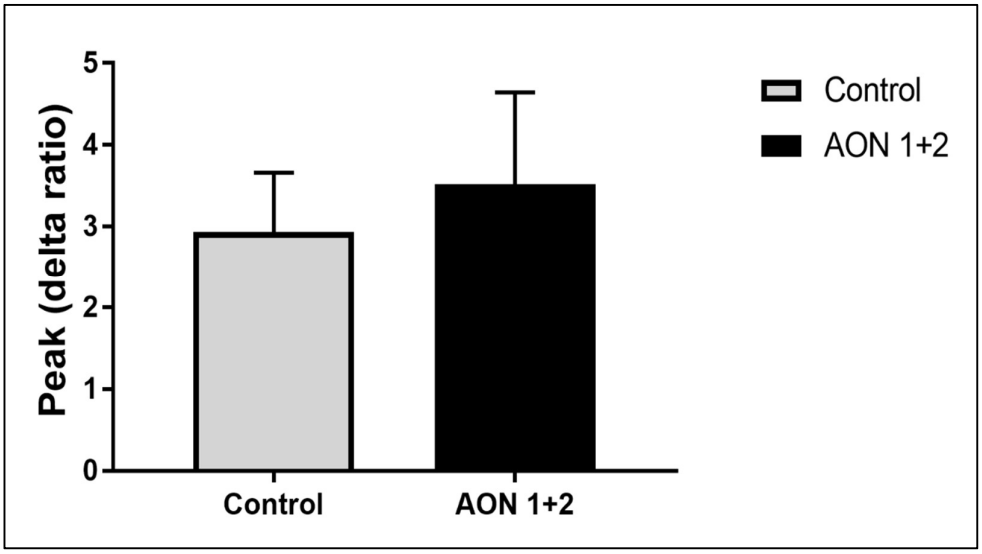

Figure 8: SOCE in AON Transfected HL-1 Cells, Peak (delta ratio/s) Arithmetic means ± SEM (n =56–60 cells) of the peak of the fluorescence ratio change seen in Figure 6 following re-addition of extracellular Ca^{2+} in AON1+2 transfected HL-1 cells (black bar) and control (grey bar). Statistical difference was tested using the two-sided Student's t-test. No significant differences were observed between groups (Hahn et al., 2019). **This figure was originally published as seen in Hahn et al., 2019.*

3.3.3 Cell Fractional Shortening of AON transfected HL-1 cells

"Finally, the ability of AON treated HL-1 cardiomyocytes to complete physiological cell contractions was evaluated by determining the cell fractional shortening by means of video-assisted planimetry. AON1+2 transfected HL-1 cell(n=20)and control cell(n=20) percent fractional shortening was calculated from the square root mean of the cell area measurements summarized from 10 continuous beats per cell" (Hahn et al., 2019).

For detailed illustrative purposes, sample images of video data from AON1+2 transfected HL-1 cells and of control HL-1 are displayed In Figures 9.1. A sample of a subsequent cell picture from the AON1+2 HL-1 cell video with a cell area marked is found in Figure 9.2. In the initial phase of this process, beating cells were identified in video data with close attention on cell borders distinguishable from other surrounding cells (depicted in Figure 9.1). Cells with prominent borders allowed for improved further cell area measurement. Pictures per frame data was then extracted and the cell area was traced, measured and noted using the programs mentioned in section 2.7 (Hahn et al., 2019).

"In our results depicted in Figure 9.3, both AON1+2 transfected HL-1 cells and control group showed an average cardiomyocyte fractional shortening of roughly 2.8%. To determine statistical difference between sample groups, a two-sided Student's t-test was performed" (Hahn et al., 2019). The Student's t-test was performed using the software GraphPad Prism(version 7.05). A difference was considered significant when $P<0.05$; no significant difference was observed (Hahn et al., 2019).

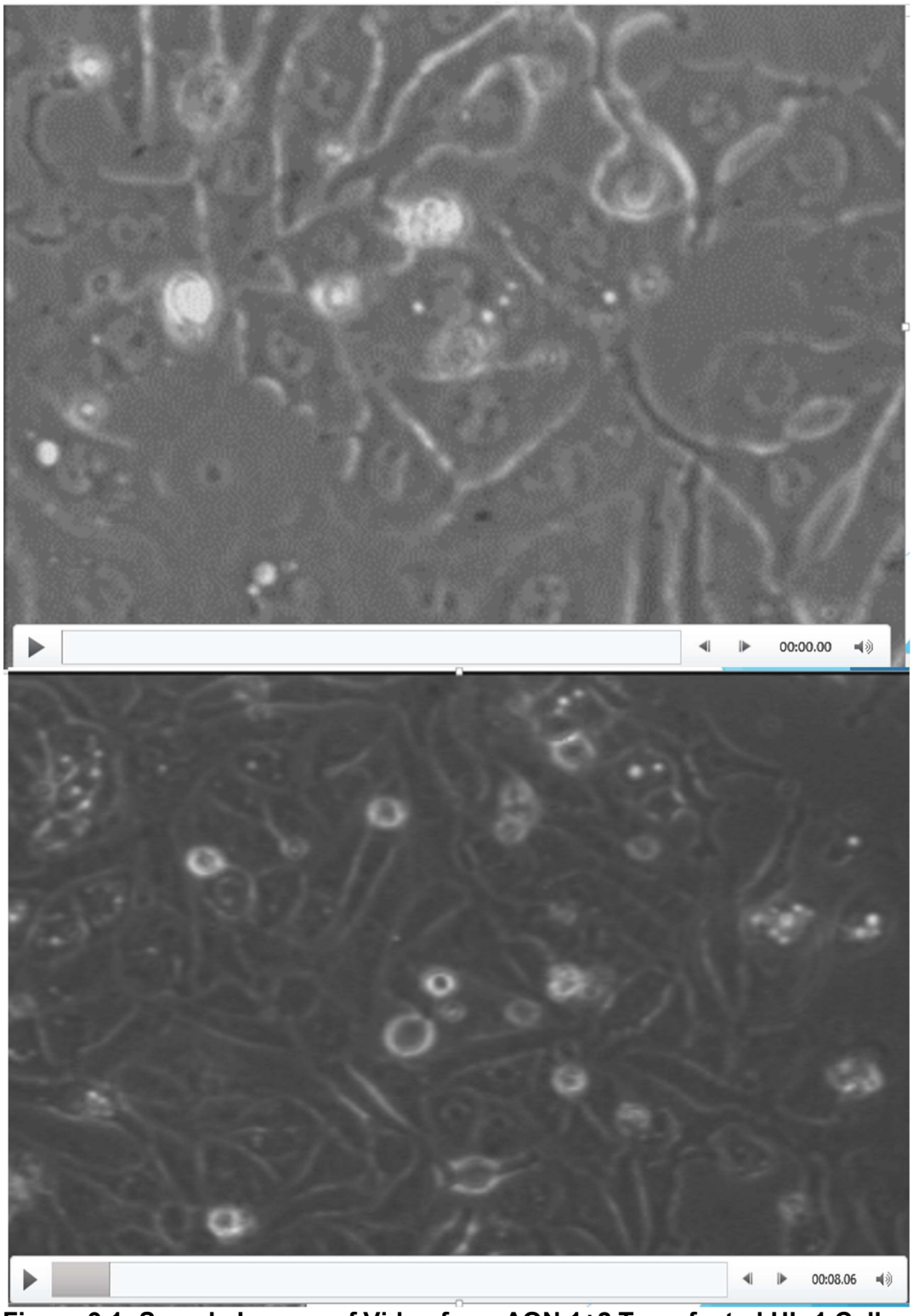

Figure 9.1: Sample Images of Video from AON 1+2 Transfected HL-1 Cells and Control HL-1 cells from Video-Assisted Cell Fractional Shortening Measurements Control HL-1 Cells (top) and AON1+2 transfected HL-1 cells (bottom) (Hahn et al., 2019).

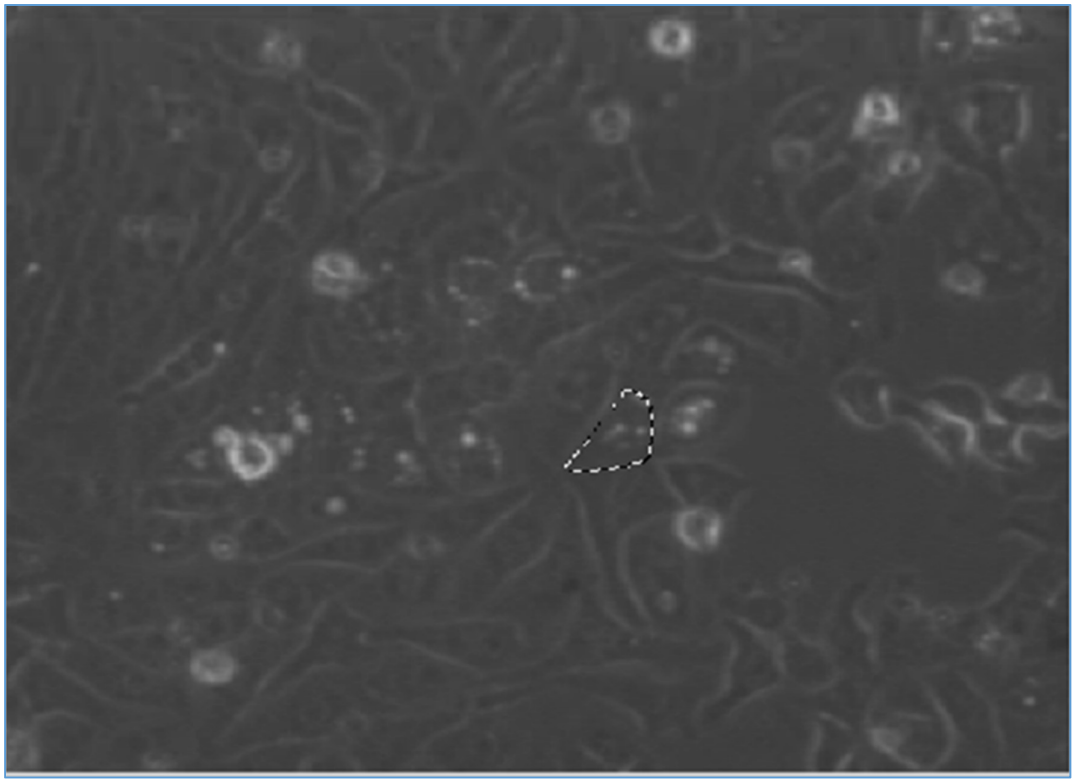

Figure 9.2 Sample Image of Picture Frame Extracted from Video in AON 1+2 Transfected HL-1 Cells for Video-Assisted Cell Fractional Shortening Measurements

Example of picture extracted from AON1+2 transfected HL-1 cells video data. Cell border of beating cell was identified, then using the trace function, outlined and area calculated using Gimp program. All cells were measured through 10 continuous beats to capture full cell contraction (see section 2.7 for detail) (Hahn et al., 2019).

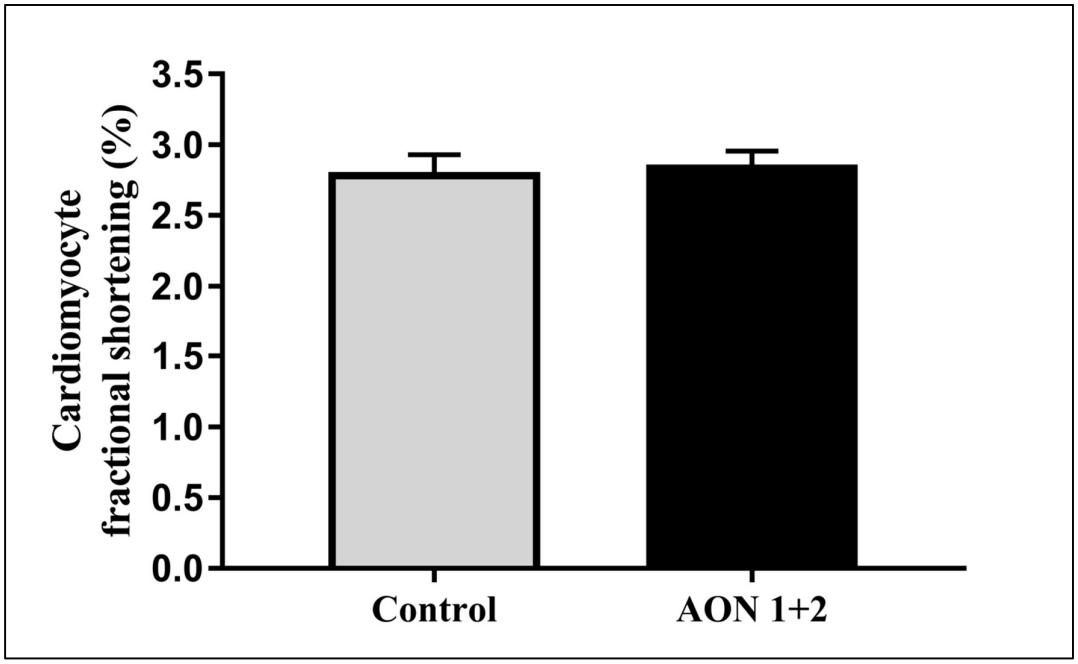

Figure 9.3: AON Transfected HL-1 Cardiomyocyte Fractional Shortening by Video-Assisted Planimetry

"AON1+2 transfected HL-1 cell(n=20)and control cell(n=20) fractional shortening illustrating cell contraction capacity. Calculations based on largest and smallest cell area attained during 10 continuous beats per cell in given sample group. Root mean square± SEM are depicted. Statistical difference was tested using the two-sided Student's t-test. No significant difference was observed between groups" (Hahn et al., 2019*).*This figure was originally published as seen in Hahn et al., 2019.*

4. Discussion

"A diverse array of genes are associated with dilated cardiomyopathy; however, remarkably, 15-20% of familial and 18% of sporadic DCM is attributed to truncating mutations in a single gene, TTN (Herman et al., 2012) (Tabish et al., 2017)(Roberts et al., 2015). TTN truncating variants can lead to frameshift mutations, resulting in shortened titin protein, altering its role in orchestrating sarcomere organization and protein signaling capabilities; these processes are assumed to contribute to the pathogenesis of DCM (Gramlich et al., 2015). A potential therapy for titin-based DCM is AON mediated exon-skipping, utilizing specifically designed RNA molecules to block incorporation of a mutated TTN exon, which aims to restore the disrupted titin reading frame with inconsequential effect on cardiomyocyte function" (Hahn et al., 2019).

"In this study, we present the first protocol to design and evaluate AONs specifically for TTN exon mutations; here, we demonstrated the successful design of two AONs with effective sequences and adequate chemistry which, when both AON1 and AON2 were combined in transient transfection, lead to validated skipping of the Ttn exon 335 in HL-1 cells without disrupting the reading frame, confirmed through direct Sanger sequencing. We further showed AON1+2 transfected HL-1 cells retained organized Z-disk protein structures (alpha-actinin and titin), calcium-stored operated entry levels and cell fractional shortening in comparison to control samples, indicating neither potential cytotoxic effects from the transfection agent polyethylenimine, nor blocking the Ttn exon 335 transcript lead to negative effects on vital cardiomyocyte sarcomeric assembly and cell processes(Khansarizadeh et al., 2015)" (Hahn et al., 2019).

"The precise mechanism of how AONs mediate exon-skipping is still not fully understood. An AON, composed of single-stranded RNA or DNA enhanced by chemical modifications, intended to block a condensed region of exonic splicing enhancer motifs, gains entry to the cell nucleus where it anneals to the target mRNA, inducing alterations to the complex splicing mechanism, leading to, for example, inclusion or exclusion of a target exon (Aartsma-Rus, 2012)(Gramlich et al., 2015). We know based on previous AON design studies, mainly focused

on the DMD gene, basic criteria should be met in order for an AON to attain potential for effective exon-skipping; however, it is important to note, even if all criteria are met, it is not fully certain that a novel AON will induce the desired effect (Aartsma-Rus, 2012). Therefore, it is essential to design multiple AONs for a given target exon to increase the chances of exon skipping taking place. In our previous work, we initially applied the mentioned criteria towards designing four different AONs to mask the ESE motifs in Ttn exon 326 and demonstrated in HL-1 cells that AONs can work harmoniously and effectively in skipping the desired exon, as well as interfere with each other in their intended function (Gramlich et al., 2015). In our current study, we aimed to further investigate the AON design and application in experiments for TTN truncating mutations causing DCM. In our studies based on TTN exon 335, we further successfully confirmed that our method yields effective exon skipping. In this case, the two AONs targeted to skip Ttn exon 335, with our preferred chemistry (2'-O-methyl RNA group, with a full-length phosphorothioate backbone), also showed synergistic activity, as only the combination of the AON1 and AON2 excluded the exon in the transcript while leaving the titin reading frame uninterrupted. In addition, upon considering the band intensity analysis results indicating 76% of the wild type Ttn exon transcript skipped, we hypothesize, with our design method and chemical modification, a considerable amount of AONs penetrated the cardiomyocytes and in combination successfully induced exon skipping in the nucleus. It would be interesting to further investigate alternate transfection methodologies with capability of enhancing the amount of desired Ttn exon transcript skipping. Taken together, these findings indicate additional TTN exons can be easily tested for exon-skipping therapeutic potential with the provided method, expanding the possibility for subsequent advanced studies in individually designed AONs for specific TTN exon mutations in DCM" (Hahn et al., 2019).

"In order to further assess the HL-1 cell capability of compensating and adapting to the exclusion of Ttn exon 335, we chose a dynamic set of measurements to best illustrate essential cardiomyocyte features which could reflect questioned cell functionality following AON treatment. Firstly, we assessed the sarcomeric structures of AON1+2 treated cells and compared results to control samples. In

immunofluorescent imagining, the Z-disk proteins alpha-actinin and titin showed conserved organization in the treated cells, implying despite the loss of Ttn exon 335 transcript, the treated cells appear to maintain sarcomeric integrity with intact coordination of sarcomerogenesis. This finding is crucial for stable cardiomyocyte myofibril survival, as alteration in the expression and thus, organization of the Z-disk region of titin, is proven to not only directly disrupt the order of the Z-disk but also indirectly affect other portions of the sarcomere such as the assembly of thick filaments into sarcomeric A-bands and actin-filaments into I-bands(Kontrogianni-Konstantopoulos et al., 2009). Secondly, as an essential mediator of cardiomyocyte contraction and protein signaling, we examined calcium influx for indication of adequate calcium homeostasis in the AON1+2 treated cells and control. In particular, we chose to evaluate the SOCE, an extracellular calcium influx pathway independent of the voltage-gated calcium channels, proven to be present in HL-1 cells and contribute to resting calcium levels (Touchberry et al., 2011). We hypothesize the SOCE function remained intact in cells following transfection, indicated by no observed statistically significant differences in comparison to control in SOCE slope and peak. Lastly, the cell fractional shortening experiment demonstrated cardiomyocyte functionality in evaluating if cells followed complete beating cycles, with comparable cell expansion and retraction. Due to no significant difference observed in cell fractional shortening between AON1+2 treated cells and the control, we assume AON treated cells were able to perform adequate cell contraction functioning as seen in healthy cardiomyocytes. Taken together, in all three investigated features, we showed AON treated cells were not negatively affected by Ttn exon 335 exclusion. We hypothesize, as also mentioned in our previous work with a similar effect observed, that the cells can compensate for the blocked exon due the modular repeating domains found in the TTN gene (Gramlich et al., 2015). This proves true for the investigated TTN exon 335, as it belongs to the large portion of TTN which is repetitive in sequence and consists of a Fn-III motif. We believe the remaining 90% mass of repetitive TTN, encoding similar motifs, compensates for the skipped exon 335; whereby, skipping of this particular exon yields normal cardiomyocyte function. The TTN exon 335 is also

ideally suitable for exon skipping as it is symmetric in structure with a nucleotide sequence divisible by three; thereby, upon its exclusion from the TTN transcript, an undisrupted reading frame would remain, as observed in our studies following sequence analysis of the AON1+2 skipped Ttn 335 transcript" (Hahn et al., 2019).

"In our previous work (Gramlich et al., 2015) we have shown that even titin's largest exon 326, which is about 17.000bp in size, can be successfully skipped using specific antisense oligonucleotides. Therefore, size should not be a limiting factor for exon skipping. However, not all of the known titin variants may be amenable to exon skipping therapy in equal ways (e.g., missense, compound heterozygous, and splicing mutations as well as variants in asymmetric exons or exons with nonredundant domains). Our work can serve as a platform for generating and evaluation the technical feasibility of AON specific skipping" (Hahn et al., 2019).

"We acknowledge one limitation of this work is the primary use of HL-1 mouse atrial cardiomyocytes as a model for the application of potential exon skipping in humans. Further investigations, for example, in a small animal model and patient-specific induced pluripotent stem cell-derived cardiomyocytes are essential to further evaluate AON exon skipping efficacy and the potential therapeutic effect" (Hahn et al., 2019).

For example, an important aspect to address is the verification that in HL-1 cells or in patient-specific iPSC-CM, an existing mutation in the exon 335 can also be successfully amenable by AON exon-skipping. It is hypothesized, the proposed method is applicable as such, as seen in previous work where initial AON-mediated skipping of Ttn exon 326 in HL-1 cardiomyocytes provided a platform to confirm cardiomyocyte compensation for the loss of the exon, followed by confirmation of sarcomeric assembly rescue in human iPSC-CM by skipping TTN exon 326 (Gramlich et al., 2015). Thus, it is believed AON exon skipping remains a strong possible therapeutic approach in titin-based DCM, where TTNtv do not completely destroy cardiomyocyte cell formation and function, leaving the opportunity for sarcomere rescue via AON exon skipping, as observed in previous studies (Gramlich et al., 2015)(Hahn et al., 2019).

"AON-mediated exon skipping aimed at reframing transcripts is an emerging and promising therapeutic strategy since the encouraging results of the phase 2/3 clinical trials for the treatment of Duchenne Muscular Dystrophy (van Deutekom et al., 2007)(Cirak et al., 2011)(Goemans et al., 2011). Our previous work shows that AON-based exon skipping is also able to prevent heart failure in a mouse model carrying a human DCM-causing TTN mutation (Gramlich et al., 2015). However, it remains unclear whether this therapy has the potential to reverse existing or sub-clinical cardiomyopathy, where structural or ultra-structural alterations may be present. Recent studies indicate that full-length titin is required for initiation of sarcomere assembly by providing basal cardiomyocyte tension, with evidence showing A-band truncations cause multiple structural sarcomeric complications (Chopra et al., 2018). TTNtv in human iPSC-CM also lead to developmental defects in sarcomere assembly and less sarcomere content (Chopra et al., 2018) (Schick et al., 2018). However, contrary to in-vitro data, carriers of TTNtv are in fact born with normal cardiac function and usually show late onset of disease (Jansweijer et al., 2017) (Roberts et al., 2015). Likewise, a titin knock-in mouse model harboring a 2 bp titin truncation mutation does not show any functional, structural or ultra-structural abnormalities under resting conditions, but requires a cardiac stressor to develop heart failure (Gramlich et al., 2009). AON-mediated exon skipping may therefore provide a therapeutic option for TTNtv carriers applied at an early age before the onset of the disease phenotype. Nonetheless, further studies are required to achieve more understanding on this matter" (Hahn et al., 2019).

An additional limitation of this work includes the narrow representation of successful exon skipping, as "*we analyzed successful exon skipping only at the RNA level" (Hahn et al., 2019).* To expand on this matter, an ideal representation of successful exon skipping in the transfected AON1+2 HL-1 cells would be more effective by also showing results of cell protein expression, where corrected protein would be also detectable, translated from successfully exon-skipped titin mRNA. In previous work performed by *Gramlich et al*, the targeted TTN exon 326 was investigated and ultimately analyzed upon exon-skipping completion on the RNA and protein level; this was achieved by implementing the Western blot

technique, as well as mass spectrometry, where a significant difference in band representation as well as corresponding peptides where observed, respectively, positively impacting result representation (Gramlich et al., 2015). However, it is important to emphasize the size difference in the investigated exons, as well as the protein titin itself. Firstly, the protein titin, "*is extremely large in size (up to 3.6MDa)* and *"the targeted exon 335 is very repetitive in structure"* this presents a challenge in *"protein expression analysis"* where skipping a single exon, small in size, would most likely prove challenging to decipher in analyzing depicted band difference in Western blotting(Hahn et al.,2019). On the other hand, during investigation of the largest TTN exon, namely exon 326, this proved possible due to the exon's much larger size. Nonetheless, protein expression analysis is an essential aspect of validating successful exon skipping and would be a supportive feature to investigate in future studies (Hahn et al., 2019)(Gramlich et al., 2015).

A further mentionable limitation of this work pertains to whether our proposed exon skipping method can, in principle, show that AON1+2 transfected HL-1 cells portray modified phenotype and thus, show desired phenotype in context of TTNtv *in vitro.* Firstly, although this work served mainly as a proposed tool to design and evaluate AONs for further disease causing TTN exons and not primarily for representation in assessment of phenotype reversibility, the reversal of phenotype remains relevant and an interesting topic of investigation. In previous work completed by *Gramlich et al*, it was shown that heart failure was preventable utilizing exon skipping in a study conducted in a mouse model carrying a DCM-causing human TTNtv (Gramlich et al., 2015). Here it was shown, titin knock-in mice, harboring a 2 base-pair-insertion mutation in the TTN exon 326, under resting conditions, did not exhibit any functional, structural or ultra-structural abnormalities in the assessment of the heart; however, DCM development did ensue upon exposition of cardiac stressors (Gramlich et al., 2015). This phenomena is similarly observed in humans, where carriers of TTNtv tend to not present with symptoms in advanced age; in addition, some carriers of TTNtv and may display complete absence of the detectable cardiac phenotype, proving even in the presence of TTNtv, the positive genotype, a

positive phenotype is not always observed (Hershberger 2019). Returning to the question of phenotypic reversal in HL-1 cells, it is unlikely a cell-line model could sufficiently provide a satisfactory result in such an investigation; it would be more suitable to perform animal and subsequent clinical studies.

Upon considering the limitations of AON design, the *"process continues to be a trail-and-error procedure, where no guarantee for exon-skipping success is momentarily attainable (Aartsma-Rus, 2012). This process could be refined to enhance maximum exon-skipping effects through a larger scale study, testing multiple AONs for other identified, mutated exons in the TTN gene. The delivery of AONs systemically with the goal of reaching and penetrating the heart muscle is not yet fully established, where a special chemistry involving cell penetrating peptides conjugated to phosphorodiamidate morpholino oligonucleotides may aide in this process(Betts et al., 2012)(Boisguérin et al., 2015)"(*Hahn et al., 2019).

Taken together, although the previously mentioned works and this study indicate exon skipping as a potential, promising future application as a therapeutic approach in titin-based DCM, it is notable to mention that there are significant advances involving exon skipping in the DMD gene, wherefrom researchers first began the idea and conception of an exon skipping therapy, by the observation of the similar, but less severe phenotype involving the DMD gene in-frame mutation causing Becker muscular dystrophy (Echevarria et al., 2018). Tremendous research advances focused on expanding exon skipping therapy for the disease Duchenne muscular dystrophy, a fatal x-linked neuromuscular disorder with devastating early life clinical manifestation of "muscle wasting" including initial ambulatory difficulty to complete loss of ambulation in teenage years, progressing to respiratory insufficiency and cardiomyopathy leading to death around age thirty, include multiple completed and existing clinical trials(Phase I-III), resulting in two FDA approved drugs(e.g. Eteplirsen, also known as "exondys 51" and Golodirsen or "Vyondys 53"), targeting exon skipping in the DMD Exon 51 and Exon 53; there are also potential additional pharmacological therapies targeted at different exons in the

DMD gene under research (Echevarria et al., 2018) (U.S. Food and Drug Administration, 2019). Similar to DCM, there is currently no cure for Duchenne muscular dystrophy, with current therapies aimed at, similar in the previously mentioned heart failure therapy, symptom reduction; here, exon skipping therapy is aimed at producing a less severe but functioning phenotype with preservation or improvement in muscle use and ambulation as seen in Becker muscular dystrophy (Echevarria et al., 2018). Although the success of Eteplirsen is not without governmental and scientific scrutiny due to small-patient group studies, narrow-spectrum patient availability and cost of the FDA approved pharmacotherapy, it would be helpful in taking a closer look at the steps leading to the current more advanced results in exon skipping therapy in the DMD gene in order to help guide further advances involving exon skipping in the TTN gene (Echevarria et al., 2018). To begin, the first AON investigated at the clinical trial level, upon success in a mouse model, targeting the human DMD Exon 51, was also designed with two chemistries, one similar to that used in the AON design mentioned in this dissertation, namely with the 2'-O-methyl phosphorothioate(2OMePS) chemistry and also with a second chemistry, namely phosphorodiamidate morpholino oligomer (PMO); the AON designed with PMO chemistry proved to be more successful producing significant results in ambulation in tested patients, which is currently known as, Eteplirsen (Echevarria et al., 2018). Upon considering the method in AON delivery, in contrast to DCM, the clinical manifestation of Duchenne muscular dystrophy presents initially in skeletal muscle, providing a definite advantage upon considering a method to test proposed pharmacotherapy, including deciphering which AON chemistry is more effective in clinical trials; this advantage allows for administration of, for example, intramuscular injections in peripheral muscle tissue such as the extensor digitorum brevis muscle, as seen in clinical trials in the testing of Eteplirsen, such injections are easily administered with minimal post-procedural complications and offer easily accessed follow-up biopsy sites(Echevarria et al., 2018). A similar method in considering the target organ of exon skipping in titin-based DCM, namely the human heart, would be primarily ethically challenging with potentially life-threating complications by

injecting the heart muscle directly with an AON sequence followed by subsequent cardiac biopsies required to investigate results. Furthermore, there are possibly significantly more severe side-effects expected from AON chemistry to deliver adequate amount of AONs in comparison to peripheral muscular injections(Echevarria et al., 2018). As such, AON delivery to the heart remains an enormous challenge not only for a clinical trial initiation in exon skipping in titin-based DCM, but also for further studies in exon skipping in Duchenne muscular dystrophy, as the disease also presents with cardiomyopathy; even with systemic administration of Eteplirsen it is yet to be shown that dystrophin expression is restored in heart tissue; here, further studies are being conducted on additional chemistry, such as peptide-conjugated PMOs, unfortunately with indications of undesirable side-effects in animal studies, however, other modified PMOs such as PMO internalization peptides (Pip) have shown more promising results, with dystophin restoration in cardiac muscle in mouse models (Echevarria et al., 2018). Nonetheless, AON delivery will remain a limitation for exon skipping therapy, which will provide an ongoing challenge as new diseases present with possible exon skipping therapy application, as such, an endless opportunity for novel AON delivery chemistry studies. A second matter to consider in comparing exon skipping in the DMD gene and the TTN gene, is the possible amount of patients who present with a rescuable genotype upon administration of exon skipping therapy. Currently, which remains one critique point of the drug Eteplirsen, aside from its extremely high cost at a list price of roughly $300,000, only around 13% of those patients affected with Duchenne muscular dystrophy can benefit from Eteplirsen, as this percent value represents approximately the amount of patients with DMD involving a mutation in the DMD Exon 51, meaning over 80% of patients diagnosed with DMD cannot benefit from Eteplirsen (Echevarria et al., 2018). Upcoming pharmacotherapies including targets for DMD Exons 45 and 53 have also met clinical trials (Echevarria et al., 2018). According to official FDA reports, as of December 2019, the exon skipping therapy targeting DMD Exon 53 known as Golodirsen or “Vyondys 53” is also officially FDA approved, providing a possible additional therapy option for approximately 8% of

remaining DMD patients who up till recently not did not benefit from the exon skipping therapy advances (U.S. Food and Drug Administration, 2019) (Echevarria et al., 2018). In regards to titin-based DCM, an exon skipping therapy targeting TTN Exon 326 could possibly provide “molecular rescue” to approximately 20% of those affected by TTN mutations causing DCM (Gramlich et al., 2015). Therefore, ongoing investigations in this therapeutic approach involved in titin-based DCM would greatly benefit a considerable amount of patients. Today, exon skipping therapies remain challenging but withhold an enormous amount of potential, offering specific, genetically designed therapies with future application not only in titin-based DCM or Duchenne muscular dystrophy but in various other disorders shown to exhibit genetic mutations leading to disease development.

The principle of exon skipping is also being applied to research conducted on numerous diseases. For example, *Shimo et al* report AON design and application of exon skipping therapies, which have successfully begun clinical trials or are nearly approaching the clinical trial phase, in the following genetic disorders: Sarcoglycanopathy, Fukuyama congenital muscular dystrophy, laminin α2 chain-deficient congenital muscular dystrophy and dysferlin-deficient muscular dystrophy (Shimo et al., 2018). Here, it is noticeable that most of the mentioned genetic disorders relate to a type of muscular dystrophy, possibly emphasizing successful application of exon skipping in genes closely related to the structural function or formation of muscle tissue. Exon skipping is, however, applicable in an abundant number of genes. For example, research focused on neurogenetic diseases, where AONs are being implemented in a “missplicing correction” therapy have also shown success in cell-line models (lymphoblastoid cell lines and patient-specific fibroblasts) involving but not limited to the following neurogenetic disesese: Ataxia telangiectasia, Niemann Pick disease type C, Neurofibromatosis 1 and Neurofibromatosis 2 (Siva et al., 2014). Hence, the future results of pending exon skipping studies will provide new insights on gene therapy application and continue to enhance alternative therapy in genetic diseases.

Finally, "*the AON-mediated exon skipping therapeutic approach in titin-based DCM is, although extensively investigated in human cell models and small animals (mouse), not yet in clinical trials. Further advanced studies are needed to approach this point of research, whereby remaining key questions, especially involving the impact of such a therapy in an existing DCM phenotype, could be elucidated"* (Hahn et al., 2019).

4.1 Conclusion

"In conclusion, in comparison to the DMD gene, few AONs are tested for the TTN gene, which is proven to be a major source of TTN truncating variants leading to the main cause of genetic DCM, currently with no curative therapy available other than heart transplantation. Here, we offer a strategy to design and evaluate AONs specifically for TTN mutations using HL-1 cells. In the future, we hope AON-mediated exon skipping can become an individualized therapeutic approach in attempts to provide an alternate therapy for titin-based dilated cardiomyopathy" (Hahn et al., 2019).

5. Summary

5.1 Summary (English Version)

Dilated cardiomyopathy is a multifactorial disease. *"The leading cause of genetic dilated cardiomyopathy (DCM) is due to mutations in the TTN gene, impacting approximately 15-20% of familial and 18% of sporadic DCM cases"* (Hahn et al.,2019). There is no specific treatment for advanced DCM, therapeutic options range from symptomatic treatment of heart failure to the indication of heart transplantation(Hahn et al.,2019).

A potential therapeutic approach for titin-based DCM is the "exon skipping" method. This is a method which utilizes RNA-based antisense-oligonucleotides (AON) to "skip" a mutated Titin exon. This method results in restoration of the previously mutated reading frame, producing a shortened but functionally intact titin protein. In past studies, we demonstrated the principle of exon skipping in cell culture and mouse models. Applying the exon skipping method in the TTN gene, comprised of 363 exons, requires specific AON design for each individual Titin exon (Gramlich et al., 2015).

This work presents*, "a detailed protocol to effectively assemble and evaluate AONs for efficient exon-skipping in targeted TTN exons"* (Hahn et al.,2019). To begin, AONs are initially designed using algorithms with the aim of skipping the chosen mutated Titin exon. Upon design completion, the AONs are transfected and tested in HL-1 cells, a mouse cardiomyocyte cell line. Confirmation of successful exon skipping of the targeted exon is then achieved utilizing RT-PCR and Sanger sequencing; in addition, the effect of exon skipping on cell functionality is further examined with immunohistochemistry, store-operated calcium entry (SOCE) and cell contractility measurements(Hahn et al.,2019).

This work is furthermore, "*the first systematic protocol in designing and evaluating AONs specifically for mutated TTN target exons, expanding the framework of future advancements in the therapeutic potential of antisense-mediated exon skipping in titin-based DCM"* (Hahn et al.,2019).

5.2 Summary (German Version)

Die dilatative Kardiomyopathie (DCM) ist eine multifaktorielle Erkrankung; ca. 15-20% der familiären und 18% der sporadischen Formen lassen sich allerdings auf Mutationen im Titin, einem Sarkomerprotein mit wichtigen Funktionen für den kontraktilen Apparat, zurückführen. Im Moment steht keine spezifische Therapie für Patienten mit fortgeschrittener DCM zur Verfügung, sodass neben symptomatischen Maßnahmen mit Behandlung der Herzinsuffizienz lediglich die Option einer Herztransplantation existiert (Hahn et al.,2019).

Ein potentieller Ansatz einer genotyp-spezifischen Therapie ist das sogenannte „Exon skipping“. Hierfür werden RNA-basierte Antisense-Oligonucleotide (AON) verwendet, um ein mutiertes Titin-Exon gezielt zu überspringen. Durch Wiederherstellung des Leserahmens entsteht ein verkürztes, aber funktionell intaktes Titin-Protein. In einer vorausgegangenen Machbarkeitsstudie haben wir das Prinzip des Exon-skippings an Zellkultur- und Mausmodell demonstrieren können. Das TTN-Gen besteht jedoch aus 363 Exonen und ist somit massiv; alle AON Sequenzen müssen deshalb für jedes einzelne Exon spezifisch entwickelt werden(Gramlich et al., 2015).

Diese Arbeit beschreibt ein Protokoll, welches für das Design und die Evaluierung von AONs für ein effizientes Exon-Skipping spezifischer TTN-Exone angewandt werden kann. Zunächst werden verschiedene in silico Algorithmen beschrieben, die putative AON Sequenzen zum Überspringen eines Titin-Exons erstellen. Anschließend werden diese AONs in transfizierten HL-1 Zellen, einer murinen Kardiomyozytenlinie, getestet. Neben dem Nachweis eines korrekten Überspringens des Target- Exons mittels RT- PCR und Sanger-Sequenzierung werden die funktionellen Auswirkungen des skippings durch Immunhistochemie, *Store-Operate-Calcium-Entry (SOCE)* und *Kontraktilitätsmessungen untersucht*(Hahn et al.,2019).

Diese Arbeit ist somit das erste systematische Protokoll zum AON-Design und deren Evaluation, um spezifische TTN Exons durch Antisense-Therapie zu

überspringen. Dies ist ein erster Schritt in Richtung einer individualisierten Therapie für die titin-basierten dilatativen Kardiomyopathie(Hahn et al.,2019).

6. Publication

Results from this dissertation are originally published in the following:

HAHN, J. K., NEUPANE, B., PRADHAN, K., ZHOU, Q., TESTA, L., PELZL, L., MALECK, C., GAWAZ, M. & GRAMLICH, M. 2019. The assembly and evaluation of antisense oligonucleotides applied in exon skipping for titin-based mutations in dilated cardiomyopathy. *J Mol Cell Cardiol*.

7. References

AARTSMA-RUS, A. 2012. Overview on AON design. *Methods Mol Biol,* 867**,** 117-29.

AARTSMA-RUS, A., FOKKEMA, I., VERSCHUUREN, J., GINJAAR, I., VAN DEUTEKOM, J., VAN OMMEN, G. J. & DEN DUNNEN, J. T. 2009. Theoretic applicability of antisense-mediated exon skipping for Duchenne muscular dystrophy mutations. *Hum Mutat,* 30**,** 293-9.

AL-MAGHOUT, T., PELZL, L., SAHU, I., SUKKAR, B., HOSSEINZADEH, Z., GUTTI, R., LAUFER, S., VOELKL, J., PIESKE, B., GAWAZ, M. & LANG, F. 2017. P38 Kinase, SGK1 and NF-κB Dependent Up-Regulation of Na⁺/Ca²⁺ Exchanger Expression and Activity Following TGFß1 Treatment of Megakaryocytes. *Cellular Physiology and Biochemistry,* 42**,** 2169-2181.

ALIGAM, E., REUTER, J. & WATSON, R.M., . 2017. *RNAstructure. Welcome to the Mathews Lab RNAstructure Web Servers* [Online]. Available: http://rna.urmc.rochester.edu/RNAstructureWeb/ [Accessed October 5, 2018].

ANON, B. 2018. *Basic Local Alignment Search Tool. National Center for Biotechnology Information* [Online]. [Accessed].

BÉROUD, C. E. A. 2010. *Human Splicing Finder Version 2.4.1. The UMD central website* [Online]. Available: http://www.umd.be/HSF/ [Accessed October 5, 2018].

BETTS, C., SALEH, A. F., ARZUMANOV, A. A., HAMMOND, S. M., GODFREY, C., COURSINDEL, T., GAIT, M. J. & WOOD, M. J. A. 2012. Pip6-PMO, A New Generation of Peptide-oligonucleotide Conjugates With Improved Cardiac Exon Skipping Activity for DMD Treatment. *Molecular Therapy. Nucleic Acids,* 1**,** e38.

BOISGUÉRIN, P., DESHAYES, S., GAIT, M. J., O'DONOVAN, L., GODFREY, C., BETTS, C. A., WOOD, M. J. A. & LEBLEU, B. 2015. Delivery of therapeutic oligonucleotides with cell penetrating peptides. *Advanced Drug Delivery Reviews,* 87**,** 52-67.

CHOPRA, A., KUTYS, M. L., ZHANG, K., POLACHECK, W. J., SHENG, C. C., LUU, R. J., . . . CHEN, C. S. (2018). Force Generation via beta-Cardiac Myosin, Titin, and alpha-Actinin Drives Cardiac Sarcomere Assembly from Cell-Matrix Adhesions. *Dev Cell, 44*(1), 87-96 e85. doi:10.1016/j.devcel.2017.12.012

CLAYCOMB, W. C., LANSON, N. A., JR., STALLWORTH, B. S., EGELAND, D. B., DELCARPIO, J. B., BAHINSKI, A. & IZZO, N. J., JR. 1998. HL-1 cells: a cardiac muscle cell line that contracts and retains phenotypic characteristics of the adult cardiomyocyte. *Proc Natl Acad Sci U S A,* 95**,** 2979-84.

ECHEVARRIA, L., AUPY, P. & GOYENVALLE, A. 2018. Exon-skipping advances for Duchenne muscular dystrophy. *Hum Mol Genet,* 27**,** R163-r172.

ELLIOTT, P., ANDERSSON, B., ARBUSTINI, E., BILINSKA, Z., CECCHI, F., CHARRON, P., DUBOURG, O., KUHL, U., MAISCH, B., MCKENNA, W. J., MONSERRAT, L., PANKUWEIT, S., RAPEZZI, C., SEFEROVIC, P., TAVAZZI, L. & KEREN, A. 2008. Classification of the cardiomyopathies: a position statement from the European Society Of Cardiology Working Group on Myocardial and Pericardial Diseases. *Eur Heart J,* 29**,** 270-6.

GARFINKEL, A. C., SEIDMAN, J. G. & SEIDMAN, C. E. 2018. Genetic Pathogenesis of Hypertrophic and Dilated Cardiomyopathy. *Heart Fail Clin,* 14**,** 139-146.

GERULL, B., ATHERTON, J., GEUPEL, A., SASSE-KLAASSEN, S., HEUSER, A., FRENNEAUX, M., MCNABB, M., GRANZIER, H., LABEIT, S. & THIERFELDER, L. 2006. Identification of a novel frameshift mutation in the giant muscle filament titin in a large Australian family with dilated cardiomyopathy. *J Mol Med (Berl),* 84**,** 478-83.

GRAMLICH, M., PANE, L. S., ZHOU, Q., CHEN, Z., MURGIA, M., SCHOTTERL, S., GOEDEL, A., METZGER, K., BRADE, T., PARROTTA, E., SCHALLER, M., GERULL, B., THIERFELDER, L., AARTSMA-RUS, A., LABEIT, S., ATHERTON, J. J., MCGAUGHRAN, J., HARVEY, R. P., SINNECKER, D., MANN, M., LAUGWITZ, K. L., GAWAZ, M. P. & MORETTI, A. 2015. Antisense-mediated exon skipping: a therapeutic strategy for titin-based dilated cardiomyopathy. *EMBO Mol Med,* 7**,** 562-76.

HAHN, J. K., NEUPANE, B., PRADHAN, K., ZHOU, Q., TESTA, L., PELZL, L., MALECK, C., GAWAZ, M. & GRAMLICH, M. 2019. The assembly and evaluation of antisense oligonucleotides applied in exon skipping for titin-based mutations in dilated cardiomyopathy. *J Mol Cell Cardiol*.

HERMAN, D. S., LAM, L., TAYLOR, M. R., WANG, L., TEEKAKIRIKUL, P., CHRISTODOULOU, D., CONNER, L., DEPALMA, S. R., MCDONOUGH, B., SPARKS, E., TEODORESCU, D. L., CIRINO, A. L., BANNER, N. R., PENNELL, D. J., GRAW, S., MERLO, M., DI LENARDA, A., SINAGRA, G., BOS, J. M., ACKERMAN, M. J., MITCHELL, R. N., MURRY, C. E., LAKDAWALA, N. K., HO, C. Y., BARTON, P. J., COOK, S. A., MESTRONI, L., SEIDMAN, J. G. & SEIDMAN, C. E. 2012. Truncations of titin causing dilated cardiomyopathy. *N Engl J Med,* 366**,** 619-28.

HERSCHBERGER, R. E., HEDGES, D. J., & MORALES, A. (2013). Dilated cardiomyopathy: the complexity of a diverse genetic architecture. *Nature Reviews Cardiology, 10*, 531. doi:10.1038/nrcardio.2013.105

HERSHBERGER, R. E. 2019. *Genetics of dilated cardiomyopathy*. UptoDate [Online]. Available: https://www.uptodate.com/contents/genetics-of-dilated-cardiomyopathy?source=history_widget. [Accessed December 8, 2019].

HERSHBERGER, R. E. 2019. *Familial dilated cardiomyopathy: Prevalence, diagnosis and treatment*. UptoDate [Online]. Available: https://www.uptodate.com/contents/familial-dilated-cardiomyopathy-prevalence-diagnosis-and-treatment?search=familial%20dilated%20cardiomyopathy&source=searc

h_result&selectedTitle=1~19&usage_type=default&display_rank=1. [Accessed January 8, 2020].

JANSWEIJER, J. A., NIEUWHOF, K., RUSSO, F., HOORNTJE, E. T., JONGBLOED, J. D., LEKANNE DEPREZ, R. H., . . . PINTO, Y. M. (2017). Truncating titin mutations are associated with a mild and treatable form of dilated cardiomyopathy. *Eur J Heart Fail, 19*(4), 512-521. doi:10.1002/ejhf.673

KIBBE, W. C., Q., . 2015. *Oligo Calc: Oligonucleotide Properties Calculator. OligoCalc: Oligonucleotide Properties Calculator* [Online]. Available: http://biotools.nubic.northwestern.edu/OligoCalc.html [Accessed October 5, 2018].

KONTROGIANNI-KONSTANTOPOULOS, A., ACKERMANN, M. A., BOWMAN, A. L., YAP, S. V. & BLOCH, R. J. 2009. Muscle Giants: Molecular Scaffolds in Sarcomerogenesis. *Physiological reviews,* 89**,** 1217-1267.

MCKENNA, W. J., MARON, B. J. & THIENE, G. 2017. Classification, Epidemiology, and Global Burden of Cardiomyopathies. *Circ Res,* 121**,** 722-730.

MANOLIO, T. A., BAUGHMAN, K. L., RODEHEFFER, R., PEARSON, T. A., BRISTOW, J. D., MICHELS, V. V., ABELMANN, W. H. & HARLAN, W. R. 1992. Prevalence and etiology of idiopathic dilated cardiomyopathy (summary of a National Heart, Lung, and Blood Institute workshop. *Am J Cardiol,* 69**,** 1458-66.

MARON, B. J., TOWBIN, J. A., THIENE, G., ANTZELEVITCH, C., CORRADO, D., ARNETT, D., MOSS, A. J., SEIDMAN, C. E. & YOUNG, J. B. 2006. Contemporary definitions and classification of the cardiomyopathies: an American Heart Association Scientific Statement from the Council on Clinical Cardiology, Heart Failure and Transplantation Committee; Quality of Care and Outcomes Research and Functional Genomics and Translational Biology Interdisciplinary Working Groups; and Council on Epidemiology and Prevention. *Circulation,* 113**,** 1807-16.

PONIKOWSKI, P., VOORS, A. A., ANKER, S. D., BUENO, H., CLELAND, J. G. F., COATS, A. J. S., FALK, V., GONZALEZ-JUANATEY, J. R., HARJOLA, V. P., JANKOWSKA, E. A., JESSUP, M., LINDE, C., NIHOYANNOPOULOS, P., PARISSIS, J. T., PIESKE, B., RILEY, J. P., ROSANO, G. M. C., RUILOPE, L. M., RUSCHITZKA, F., RUTTEN, F. H. & VAN DER MEER, P. 2016. 2016 ESC Guidelines for the diagnosis and treatment of acute and chronic heart failure: The Task Force for the diagnosis and treatment of acute and chronic heart failure of the European Society of Cardiology (ESC)Developed with the special contribution of the Heart Failure Association (HFA) of the ESC. *Eur Heart J,* 37**,** 2129-2200.

PRAMONO, Z. A., WEE, K. B., WANG, J. L., CHEN, Y. J., XIONG, Q. B., LAI, P. S. & YEE, W. C. 2012. A prospective study in the rational design of

efficient antisense oligonucleotides for exon skipping in the DMD gene. *Hum Gene Ther,* 23**,** 781-90.

Report of the WHO/ISFC task force on the definition and classification of cardiomyopathies. *Br Heart J 1980,* 44**,** 672-3.

ROBERTS, A. M., WARE, J. S., HERMAN, D. S., SCHAFER, S., BAKSI, J., BICK, A. G., BUCHAN, R. J., WALSH, R., JOHN, S., WILKINSON, S., MAZZAROTTO, F., FELKIN, L. E., GONG, S., MACARTHUR, J. A., CUNNINGHAM, F., FLANNICK, J., GABRIEL, S. B., ALTSHULER, D. M., MACDONALD, P. S., HEINIG, M., KEOGH, A. M., HAYWARD, C. S., BANNER, N. R., PENNELL, D. J., O'REGAN, D. P., SAN, T. R., DE MARVAO, A., DAWES, T. J., GULATI, A., BIRKS, E. J., YACOUB, M. H., RADKE, M., GOTTHARDT, M., WILSON, J. G., O'DONNELL, C. J., PRASAD, S. K., BARTON, P. J., FATKIN, D., HUBNER, N., SEIDMAN, J. G., SEIDMAN, C. E. & COOK, S. A. 2015. Integrated allelic, transcriptional, and phenomic dissection of the cardiac effects of titin truncations in health and disease. *Sci Transl Med,* 7**,** 270ra6.

SCHAFER, S., DE MARVAO, A., ADAMI, E., FIEDLER, L. R., NG, B., KHIN, E., RACKHAM, O. J., VAN HEESCH, S., PUA, C. J., KUI, M., WALSH, R., TAYAL, U., PRASAD, S. K., DAWES, T. J., KO, N. S., SIM, D., CHAN, L. L., CHIN, C. W., MAZZAROTTO, F., BARTON, P. J., KREUCHWIG, F., DE KLEIJN, D. P., TOTMAN, T., BIFFI, C., TEE, N., RUECKERT, D., SCHNEIDER, V., FABER, A., REGITZ-ZAGROSEK, V., SEIDMAN, J. G., SEIDMAN, C. E., LINKE, W. A., KOVALIK, J. P., O'REGAN, D., WARE, J. S., HUBNER, N. & COOK, S. A. 2017. Titin-truncating variants affect heart function in disease cohorts and the general population. *Nat Genet,* 49**,** 46-53.

SHIMO, T., MARUYAMA, R. & YOKOTA, T. 2018. Designing Effective Antisense Oligonucleotides for Exon Skipping. *In:* BERNARDINI, C. (ed.) *Duchenne Muscular Dystrophy: Methods and Protocols.* New York, NY: Springer New York.

SIVA, K., COVELLO, G. & DENTI, M. A. 2014. Exon-skipping antisense oligonucleotides to correct missplicing in neurogenetic diseases. *Nucleic Acid Ther,* 24**,** 69-86.

SQUIRE, J. M. 1997. Architecture and function in the muscle sarcomere. *Current Opinion in Structural Biology,* 7**,** 247-257.

SYED, Y. Y. 2016. Eteplirsen: First Global Approval. *Drugs,* 76**,** 1699-1704.

TABISH, A. M., AZZIMATO, V., ALEXIADIS, A., BUYANDELGER, B. & KNÖLL, R. 2017. Genetic epidemiology of titin-truncating variants in the etiology of dilated cardiomyopathy. *Biophysical Reviews***,** 1-17.

TAYAL, U., PRASAD, S., & COOK, S. A. (2017). Genetics and genomics of dilated cardiomyopathy and systolic heart failure. *Genome Medicine, 9*(1), 20. doi:10.1186/s13073-017-0410-8

TOUCHBERRY, C. D., ELMORE, C. J., NGUYEN, T. M., ANDRESEN, J. J., ZHAO, X., ORANGE, M., WEISLEDER, N., BROTTO, M., CLAYCOMB, W. C. & WACKER, M. J. 2011. Store-operated calcium entry is present in

HL-1 cardiomyocytes and contributes to resting calcium. *Biochemical and biophysical research communications,* 416**,** 45-50.

U.S. Food and Drug Administration. (2019). *Drug Trials Snapshots: VYONDYS 53*. [online] Available at: https://www.fda.gov/drugs/drug-approvals-and-databases/drug-trials-snapshots-vyondys-53 [Accessed 11 Jan. 2020].

WEIGNER, M., MORGAN, J. P. (2019). *UpToDate*. [online] Uptodate.com. Available at: https://www.uptodate.com/contents/causes-of-dilated-cardiomyopathy?search=DCM&source=search_result&selectedTitle=1~25&usage_type=default&display_rank=1 [Accessed 5 Oct. 2019].

WILTON, S. D., FALL, A. M., HARDING, P. L., MCCLOREY, G., COLEMAN, C. & FLETCHER, S. 2007. Antisense oligonucleotide-induced exon skipping across the human dystrophin gene transcript. *Mol Ther,* 15**,** 1288-96.

ZERBINO, D. R., ACHUTHAN, P., AKANNI, W., AMODE, M R., BARRELL, D., BHAI, J., BILLIS, K., CUMMINS, C., GALL, A., GIRÓN, C. G., GIL, L., GORDON, L., HAGGERTY, L., HASKELL, E., HOURLIER, T., IZUOGU, O. G., JANACEK, S. H., JUETTEMANN, T., TO, J. K., LAIRD, M. R., LAVIDAS, I., LIU, Z., LOVELAND, J. E., MAUREL, T., MCLAREN, W., MOORE, B., MUDGE, J., MURPHY, D. N., NEWMAN, V., NUHN, M., OGEH, D., ONG, C. K., PARKER, A., PATRICIO, M., RIAT, H. S., SCHUILENBURG, H., SHEPPARD, D., SPARROW, H., TAYLOR, K., THORMANN, A., VULLO, A., WALTS, B., ZADISSA, A., FRANKISH, A., HUNT, S. E., KOSTADIMA, M., LANGRIDGE, N., MARTIN, F. J., MUFFATO, M., PERRY, E., RUFFIER, M., STAINES, D. M., TREVANION, S. J., AKEN, B. L., CUNNINGHAM, F., YATES, A. & FLICEK, P. 2018. Ensembl 2018. *Nucleic Acids Research,* 46**,** D754-D761.

Supplementary Information

Designed AON Sequences (Hahn et al., 2019)

Name	Sequence
AON1	UAGGUCGAUUUCUGGUUCCU
AON2	CAGUAGUUGGACAUCUUCAC

GTATGTACCTACTGGTTTGATTATGTTTTTTAATAAGCATACTTCCAGGAAA
TCACTCTTTTTTGCTTTTAAAATTCACTGTATGTATCCATTTTATGTCT
ACAGAGGCACCAGAGATTGACCTGGATGTGGCTCTCAGAACTTCTGTTATT
GCCAAAGCTGGTGAAGATGTACAAGTGTTGATTCCCTTTAAAGGCAGACCT
CCACCTACTGTCACATGGAGAAAAGATGAGAAGAATCTTGGCAGTGATGC
CAGATACAGCATTGAAAACACTGATTCATCCTCATTACTCACCATTCCTCAA
GTTACTCGCAATGATACAGGAAAATATATTCTCACAATAGAAAATGGAGTTG
GTGAACCTAAGTCTTCAACTGTGAGTGTTAAAGTGCTTGACACACCAGCTG
CCTGCCAGAAACTACAGGTTAAACATGTTTCTCGAGGCACAGTCACTTTGC
TCTGGGATCCTCCTCTCATTGATGGAGGATCTCCAATAATTAATTATGTCAT
TGAAAAGAGAGATGCCACCAAGAGAACATGGTCTGTCGTGTCACACAAAT
GTTCTAGCACATCCTTCAAGCTAATAGATTTGTCGGAGAAGACTCCATTCTT
CTTCAGAGTTCTTGCAGAAAATGAAATTGGAATTGGGGAACCCTGTGAAAC
TACAGAGCCAGTGAAGGCTGCTGAAGTACCAGCTCCTATACGTGATCTCTC
AATGAAAGACTCAACAAAGACATCTGTCATCCTCAGCTGGACCAAACCTGA
CTTTGATGGTGGTAGCGTCATCACAGAATATGTTGTAGAAAGGAAAGGTAA
AGGTGAACAGACGTGGTCCCACGCTGGCATAAGTAAGACATGTGAAATTG
AGGTTAGCCAACTTAAGGAGCAGTCAGTCCTGGAGTTCAGAGTGTTTGCC
AAAAATGAGAAAGGACTGAGTGATCCTGTCACTATTGGGCCAATTACAGTG
AAAGAACTTATTATTACACCTGAAGTTGACCTGTCAGATATCCCTGGGGCA
CAAGTCACTGTGAGAATTGGGCACAATGTGCACCTTGAATTACCTTATAAG
GGAAAACCCAAACCATCCATCAGTTGGCTGAAAGATGGCTTGCCACTGAAA
GAAAGTGAATTTGTTCGCTTCAGTAAAACTGAAAACAAAATTACTTTGAGTA
TTAAGAATGCCAAGAAGGAGCATGGAGGAAAATACACTGTTATTCTTGATA
ATGCAGTGTGTAGAATTGCAGTCCCCATTACAGTCATCACCCTTGGCCCAC
CATCAAAGCCCAAAGGACCCATTCGATTTGATGAAATCAAGGCTGATAGTG
TCATCCTGTCATGGGATGTACCTGAAGATAATGGAGGAGGAGAAATTACTT
GTTACAGCATCGAGAAGCGGGAAACTTCACAAACTAACTGGAAGATGGTG
TGTTCAAGTGTTGCCAGAACGACTTTCAAAGTTCCTAATCTAGTCAAAGATG
CTGAGTACCAGTTTAGAGTGAGAGCAGAAAACAGATACGGAGTCAGCCAA
CCACTTGTCTCAAGCATTATTGTGGCAAAACACCAGTTCAGGATTCCTGGT
CCCCCAGGAAAGCCAGTTATATACAATGTGACTTCTGATGGCATGTCACTA
ACTTGGGATGCTCCAGTTTATGATGGTGGTTCAGAAGTTACTGGATTCCAT
GTTGAAAAGAAAGAAAGAAATAGCATCCTCTGGCAAAAAGTTAATACATCA
CCAATCTCTGGAAGAGAATATAGAGCCACTGGACTGGTAGAAGGTCTGGA
TTACCAATTCCGTGTATATGCTGAAAATTCTGCTGGCCTAAGCTCACCTAGT
GACCCAAGCAAATTTACCTTAGCTGTTTCTCCAGTAG

Figure 2.1: Human TTN Intron 334 and Exon 335
Human TTN intron(in grey) and exon(black) sequences gathered from the Ensembl website; this sequence data was used to compare to and identify accurate mouse exon sequence for AON design(Zerbino et al., 2018). Samples of similar sequence pattern to mouse exon sequence in Figure 2.2 are underlined (Hahn et al., 2019).

ACTCATTTTCTTTTAAAACTCACGGTAAATGTCUGTTTTT GTGUCT
ACAGAGGAACCAGAAATCGACCTAGATGTGGCTCTCAGAACATCTGTTATA
GCTAAAGCTGGTGAAGATGTCCAACTACTGATTCCCTTTAAAGGCAGACCG
CCACCTACTGTCACCTGGAGGAAAGATGAGAAGAATCTTGGCAGCGATACC
AGATACAGCATCCAAAACACTGATTCGTCTTCTTTGCTTGTTATTCCTCAAGT
CACTCGCAATGATACAGGAAAATACATCCTGACAATAGAAAACGGAGTAGGC
CAACCAAAGTCTTCCACCGTGAGTGTTAAGGTGCTCGACACACCAGCTGC
CTGCCAGAAGTTACAGGTGAAACATGTTTCCCTAGGCACAGTCACATTGCT
CTGGGATCCTCCTCTCATCGATGGAGGGTCTCCCATCATTAACTATGTCATC
GAAAAGAGAGATGCCACGAAGAGAACATGGTCTGTTGTGTCACACAAGTGT
TCCGGCACATCCTTTAAAGTAACAGATTTATCAGAGAAGACTCCATTCTTCTT
CAGGGTTCTTGCAGAAAATGAAATTGGCATTGGTGAGCCTTGCGAGACCAC
GGAGCCCGTGAAGGCTGCTGAGGTGCCAGCACCTATCCGAGATCTCTCAA
TGAAAGATTCCACAAAGACATCTGTTGTCCTGAGCTGGACCAAGCCTGACT
TTGATGGTGGGAGCATCATCACAGACTATCTGGTGGAACGGAAAGGCAAAG
GTGAACAAGCATGGTCCCATGCTGGCATCAGTAAGACATGTGAGATTGAGA
TTGGACAACTTAAAGAGCAATCAGTCTTGGAATTCCGAGTGTCTGCTAGAAA
TGAGAAAGGACAGAGCGACCCTGTCACTATTGGGCCACTTACAGTGAAGG
AGCTTGTAATTACACCTGAAGTTGACTTGTCAGAAATCCCTGGGGCACAAAT
ATCTGTGAGAATTGGACATAACGTACACCTTGAATTACCTTATAAAGGAAAAC
CCAAGCCATCCATCAGTTGGCTGAAAGATGGCTTGCCACTGAAGGAAAGTG
AATATGTTCGTTTCAGTAAGACAGAAAACAAAATCACCTTGAGTATTAAGAAT
TCGAAGAAAGAGCATGGAGGGAAATATACTGTTATTCTTGATAATGCAGTGT
GTAGAAACTCATTCCCCATTACAATCATCACCCTCGGCCCACCGTCAAAGC
CCAAAGGACCCATTAGATTTGATGAAATCAAGGCTGACAGCGCCATCATGT
CATGGGACATACCTGAAGATGACGGAGGAGGAGAAATCACCTGTTACAGCA
TTGAGAAGCGGGAAGCATCACAAACAAATTGGAAGATGGTGTGTTCAAGTG
TTGCCAGAACAACTTTCAAAGTTTCCAATCTGGTCAAAGATTCTGAATACCA
GTTTAGAGTTAGAGCAGAAAATAGATATGGAGTCAGTGAGCCACTTGCCTCA
AATATCATCGTGGCAAAACACCAATTCAGGATTCCTGGTCCTCCAGGAAAG
CCAGTCATCTACAATGTAACTTCGGATGGCATGTCACTAACTTGGGATGCAC
CAGTTTATGATGGTGGTTCAGAAGTTACTGGATTCCATGTTGAAAAGAAAGA
AAGAAACAGCATTCTTTGGCAAAGGGTTAACACATCACCAATATCTGGGAGA
GAATACAGAGCTACTGGCTTAATAGAAGGGCTGGACTATCAATTCCGTGTAT
ATGCTGAGAATTCTGCTGGCCTGAGCTCACCTAGTGACCCAAGCAAGTTTA
CATTAGCTGTTTCCCCAGTAG

Figure 2.2: Mouse Exon sequence corresponding to TTN Intron 334 and Exon 335

Exon sequence of *Ttn* intron 334(grey) and *Ttn* exon 335(black) gathered from the Ensembl website; this sequence data was used to compare to and identify the accurate mouse exon sequence for AON design (Zerbino et al., 2018). Samples of similar sequence pattern to human exon sequence in Figure 2.1 are underlined (Hahn et al., 2019).

ACUCAUUUUC UUUUAAAACU CACGGUAAAU GUCUGUUUUU
GUGUCUACAG **AGGAACCAGA AAUCGACCUA** GAUGUGGCUC
UCAGAACAUC UGUUAUAGCU AAAGCUG**GUG AAGAUGUCCA**
ACUACUGAUU CCCUUUAAAG GCAGACCGCC ACCUACUGUC
ACCUGGAGGA AAGAUGAGAA GAAUCUUGGC AGCGAUACCA

GAUACAGCAU CCAAAACACU GAUUCGUCUU CUUUGCUUGU
UAUUCCUCAA GUCACUCGCA AUGAUACAGG AAAAUACAUC
CUGACAAUAG AAAACGGAGU AGGCCAACCA AAGUCUUCCA
CCGUGAGUGU UAAGGUGCUC GACACACCAG CUGCCUGCCA
GAAGUUACAG GUGAAACAUG UUUCCCUAGG CACAGUCACA

UUGCUCUGGG AUCCUCCUCU CAUCGAUGGA GGGUCUCCCA
UCAUUAACUA UGUCAUCGAA AAGAGAGAUG CCACGAAGAG
AACAUGGUCU GUUGUGUCAC ACAAGUGUUC CGGCACAUCC
UUUAAAGUAA CAGAUUUAUC AGAGAAGACU CCAUUCUUCU
UCAGGGUUCU UGCAGAAAAU GAAAUUGGCA UUGGUGAGCC

UUGCGAGACC ACGGAGCCCG UGAAGGCUGC UGAGGUGCCA
GCACCUAUCC GAGAUCUCUC AAUGAAAGAU UCCACAAAGA
CAUCUGUUGU CCUGAGCUGG ACCAAGCCUG ACUUUGAUGG
UGGGAGCAUC AUCACAGACU AUCUGGUGGA ACGGAAAGGC
AAAGGUGAAC AAGCAUGGUC CCAUGCUGGC AUCAGUAAGA

Figure 2.3: Exact *Ttn* intron 334 *and Ttn* exon 335 Nucleotide Sequence used for AON Design
Nucleotide sequence of corresponding mouse intron TTN 334 and exon TTN 335. Here in grey depicted, the last 50 nucleotides of *Ttn* exon 334 and in black the first 150 nucleotides of *Ttn* 335. First and second target sequence zones bold and underlined (Hahn et al., 2019). Sequence information gathered from the Ensembl website, release version 93(Zerbino et al., 2018).

Reagents

Cell culture:

Claycomb Medium	SAFC Biosciences, Kansas, USA
Fetal Bovine Serum	Sigma-Aldrich, St. Louis, USA
Norepinephrine	Sigma-Aldrich, St. Louis, USA
L-Ascorbic Acid, Sodium Salt	Sigma-Aldrich, St. Louis, USA
L-Glutamine	Sigma-Aldrich, St. Louis, USA
Trypsin-EDTA	PAA, Pasching, Austria
Dulbecco's PBS (Ca2+-free and Mg2+-free)	PAA, Pasching, Austria
Fibronectin	Sigma-Aldrich, St. Louis, USA
Gelatin from Bovine Skin	Sigma-Aldrich, St. Louis, USA
Cell Culture Grade Cryovials	Greiner Bio-one, Frickenhausen, Germany
Sterile Acrodisc Syringe Filters, 0.2µm	Merck Millipore, Darmstadt, Germany
PEI Transfection Reagent	Sigma-Aldrich, St. Louis, USA

Other Reagents:

Formamide	Carl Roth, Karlsruhe, Germany
4% PFA	Otto Fischar, Saarbruecken, Germany
Triethanolamine	Sigma-Aldrich, St. Louis, USA
Acetic anhydride	Sigma-Aldrich, St. Louis, USA
Denhardts Solution (5x)	Affymetrix, Santa Clara, USA
H2O2	Merck Millipore, Darmstadt, Germany
DAPI	Sigma-Aldrich, St. Louis, USA
DMSO	Sigma-Aldrich, St. Louis, USA

Author Contribution

This work was performed in the Department of Cardiology and Cardiovascular Diseases, Eberhard Karls University (Medizinische Universitätsklinik Tübingen aus der Abteilung Innere Medizin III –Kardiologie und Kreislauferkrankungen) under the supervision of Prof. Dr. med. Michael Gramlich and further assistance from PhD Student, Mr. Qifeng Zhou and Dr. rer.nat. Balram Neupane.

Prof. Dr. med. Michael Gramlich, Mr. Qifeng Zhou and myself developed the concept of this work and designed experiments.

Mr. Qifeng Zhou and I designed the antisense oligonucleotides and completed the laboratory experiments together, with the exception of the calcium experiments.

All cell preparations for calcium experiments were performed by myself; the SOCE measurements, written method description and illustrations (Figures 6-8) were created by Dr.rer.nat.Lisann Pelzl in the Department of Physiology I, Eberhard Karls University.

Cell measurements from the video files of transfected cells were performed by Ms. Lauren Testa (Bachelor Student, RISE Program); data analysis was completed by myself.

All text, literature research, remaining illustrations and tables involved with this work and the corresponding listed publication were performed solely by me with the exception of the following: 1) The 7th paragraph of the discussion section was collectively constructed by Prof. Dr. med Gramlich, Dr. Neupane and myself 2) Calcium measurements and method were completed Dr.rer.nat.Lisann Pelzl 3) Illustration editing and statistics were completed by Dr.rer.nat.Balram Neupane 4) Figure 1.0 is an original graphic from *Gramlich et al., 2015*; permission to display this was granted by Univ.-Prof. Dr. med.

Michael Gramlich. These contributions also apply to the publication derived from this work.

The scope of this manuscript was guided by Prof. Dr. med. Michael Gramlich.

Prof. Dr. med. Michael Gramlich and Dr. rer.nat. Balram Neupane assisted in proof-reading this manuscript for accuracy and completeness.

Acknowledgements

I would like to thank Prof. Dr. med. Michael Gramlich for giving me the opportunity to work on this research topic and for organizing the means for the project funding.

I also would also like to thank Mr. Qifeng Zhou, Dr.rer.nat. Balram Neupane, Dr. Parwez Aidery, Dr.rer.nat. Lisann Pelzl and the lab members in our department who offered their support and assistance in various ways to help see this project succeed.

Finally, I would like to thank my parents, Jeffrey and Susan Hahn, along with my entire family, for their unconditional encouragement and support spanning from the first day of laboratory work until the last written page of this manuscript.